NBS TECHNICAL NOTE **594-14**

Optical Radiation Measurements:

High Pressure Sodium Discharge Lamp Characterization for Use as Standards of Geometrically Total Luminous Flux

Minggao He and Robert J. Bruening

*T*he National Bureau of Standards[1] was established by an act of Congress on March 3, 1901. The Bureau's overall goal is to strengthen and advance the Nation's science and technology and facilitate their effective application for public benefit. To this end, the Bureau conducts research to assure international competitiveness and leadership of U.S. industry, science and technology. NBS work involves development and transfer of measurements, standards and related science and technology, in support of continually improving U.S. productivity, product quality and reliability, innovation and underlying science and engineering. The Bureau's technical work is performed by the National Measurement Laboratory, the National Engineering Laboratory, the Institute for Computer Sciences and Technology, and the Institute for Materials Science and Engineering.

The National Measurement Laboratory

Provides the national system of physical and chemical measurement; coordinates the system with measurement systems of other nations and furnishes essential services leading to accurate and uniform physical and chemical measurement throughout the Nation's scientific community, industry, and commerce; provides advisory and research services to other Government agencies; conducts physical and chemical research; develops, produces, and distributes Standard Reference Materials; provides calibration services; and manages the National Standard Reference Data System. The Laboratory consists of the following centers:

- Basic Standards[2]
- Radiation Research
- Chemical Physics
- Analytical Chemistry

The National Engineering Laboratory

Provides technology and technical services to the public and private sectors to address national needs and to solve national problems; conducts research in engineering and applied science in support of these efforts; builds and maintains competence in the necessary disciplines required to carry out this research and technical service; develops engineering data and measurement capabilities; provides engineering measurement traceability services; develops test methods and proposes engineering standards and code changes; develops and proposes new engineering practices; and develops and improves mechanisms to transfer results of its research to the ultimate user. The Laboratory consists of the following centers:

- Computing and Applied Mathematics
- Electronics and Electrical Engineering[2]
- Manufacturing Engineering
- Building Technology
- Fire Research
- Chemical Engineering[3]

The Institute for Computer Sciences and Technology

Conducts research and provides scientific and technical services to aid Federal agencies in the selection, acquisition, application, and use of computer technology to improve effectiveness and economy in Government operations in accordance with Public Law 89-306 (40 U.S.C. 759), relevant Executive Orders, and other directives; carries out this mission by managing the Federal Information Processing Standards Program, developing Federal ADP standards guidelines, and managing Federal participation in ADP voluntary standardization activities; provides scientific and technological advisory services and assistance to Federal agencies; and provides the technical foundation for computer-related policies of the Federal Government. The Institute consists of the following divisions:

- Information Systems Engineering
- Systems and Software Technology
- Computer Security
- Systems and Network Architecture
- Advanced Systems

The Institute for Materials Science and Engineering

Conducts research and provides measurements, data, standards, reference materials, quantitative understanding and other technical information fundamental to the processing, structure, properties and performance of materials; addresses the scientific basis for new advanced materials technologies; plans research around cross-cutting scientific themes such as nondestructive evaluation and phase diagram development; oversees Bureau-wide technical programs in nuclear reactor radiation research and nondestructive evaluation; and broadly disseminates generic technical information resulting from its programs. The Institute consists of the following divisions:

- Ceramics
- Fracture and Deformation[3]
- Polymers
- Metallurgy
- Reactor Radiation

[1]Headquarters and Laboratories at Gaithersburg, MD, unless otherwise noted; mailing address Gaithersburg, MD 20899.
[2]Some divisions within the center are located at Boulder, CO 80303.
[3] Located at Boulder, CO, with some elements at Gaithersburg, MD.

Optical Radiation Measurements:

High Pressure Sodium Discharge Lamp Characterization for Use as Standards of Geometrically Total Luminous Flux

Minggao He

Fudan University
Shanghai, China

Robert J. Bruening

Center for Radiation Research
National Measurement Laboratory
National Bureau of Standards
Gaithersburg, MD 20899

Abstract

The stability of commercial 400W high pressure sodium lamps has been studied to allow the selection of lamps that produce a stable luminous flux on relighting. The properties of the lamps have been studied during the first minutes of starting, their output on relighting in place, and their output after 100's of hours burning. Lamps have been selected that repeat to $\pm$ 1% on relighting, and are expected to remain that stable over a life of about 450 hours. The lamps have been calibrated for total luminous flux by sphere comparison, with an uncertainty of $\pm$4.6%. These lamps will be used as working standards, and goniometric measurements will be made to reduce the uncertainty.

TABLE OF CONTENTS

1. Introduction

The National Bureau of Standards has provided standards for measurements of light for much of its history. Photometric standards have been issued in the form of calibrated incandescent tungsten lamps. Such lamps were quite satisfactory for many years when the bulk of lighting was provided by tungsten illumination, having similar spectral properties to the standards. Over the years, discharge lamps have come into very common use. However, such lamps have spectral distributions that are quite different from that of a tungsten lamp. Calibration of the luminous flux produced by a discharge lamp by direct photometric comparison to a tungsten lamp standard can not be made with the same accuracy as that available for tungsten lamp to tungsten lamp comparisons. Therefore, modern lighting laboratories calibrate discharge lamps by making spectral measurements of the lamp output. The lighting industry has asked the NBS to produce standards which would be calibrated spectrally, and to provide a discharge type of calibrated lamp which more closely matches the type of lamp and method of calibration used in industry. A high pressure sodium discharge lamp (HPS) was chosen for this standard. The stability of the light output of 400W HPS lamps has been studied, and as a result, methods have been developed to select the most stable lamps for calibration as standards.

2. Development of HPS lamp

High pressure sodium (HPS) lamps provide an economical source of illumination. Introduced by Louden and Schmidt [1] in 1965, such lamps generate light by an electric discharge in sodium vapor. They convert electricity into light more efficiently than incandescent, fluorescent, or other discharge light sources, producing the highest luminous efficacy of all short arc high intensity discharge (HID) light sources. The luminous efficacy of HPS lamp can be as high as 150 lm/W [2]. This is six times the efficacy of typical incandescent lamps, over twice the efficacy of high pressure mercury lamps, and about 50% higher than the efficacy of either metal halide or fluorescent lamps. Over the twenty years since their initial development, the HPS lamp has been improved by research into the basic properties of electrical discharge in sodium vapor at high pressures. Comprehensive review papers on HPS lamps [3, 4, 5, 6] have reported on both basic and engineering aspects of the development. In such lamps, the high pressure sodium vapor discharge arc operates at temperatures of up to 1500°C, producing optical radiation with a broadened spectrum near the peak of the human eye photopic vision.

With continued development of new materials and technology, this lamp may come close to its theoretical maximum efficacy of 385 lm/W. For a conventional 400W HPS lamp, the efficacy including ballast losses, is presently about 120 lm/W. Like other HID lamps, the efficacy increases with increasing wattage. They have a very long life, about 24,000 hours on average, and a correlated color temperature of about 2100 K. Unlike the metal halide lamps, the flux output of HPS lamps is not affected by the burning position or tilt angle. The major hindrance to wide use of

1

HPS lamps is their poor color rendering of everyday objects, since HPS lamps have a color rendering index (CRI) of approximately 25 [7].

HPS lamps have become the most popular ·HID source for general outdoor lighting applications such as roadway lighting, tunnel lighting, area lighting and building floodlighting. HPS lamps are also rapidly becoming the economical choice for many stadium lighting needs. For indoor lighting, there is an increasing interest in their application to commercial, industrial, school, and sports areas where high efficacy is of prime importance and color rendition is a secondary consideration.

There are proven techniques that will improve the color rendering index of HPS lamps. These techniques include increasing the sodium operating pressure to emphasize the self-absorption and re-emission of the D-lines, using additives in the lamp to provide spectra other than that from sodium, or exciting higher energy levels of the sodium vapor to obtain emission at wavelengths other than the D-lines [3].

In the past years, using these methods, lamp manufacturers have developed some ultra-HPS lamps with an improved color rendering index, but only at the expense of luminous efficacy. At present, new HPS lamps with superior color rendering properties and high efficacy have been developed by several researchers. Bhalla, et al, [8] realized the new 250W HPS lamps with a CRI of 65 and an efficacy of 100 lm/W, and Otani, et al, [2] developed a new type of retrofit HPS lamp which achieves an improved CRI of 50-60 with high luminous efficacy of 105-130 lm/W (220W-660 W). Akutsu, et al, [9] described their improvement of new 150W-400W HPS lamps with CRI of 78-85, a luminous efficacy of 40-60 lm/W, an average life time of 9,000 hrs., and a correlated color temperature between 2500K and 2800K, close to that of an incandescent lamp. Because of their higher CRI, higher efficacy, and longer life than incandescent lamps, the new HPS lamps have achieved widespread commercial importance for many lighting purposes where color rendition (illuminating quality) are needed. They provide comfortable lighting environments with an energy-saving substitute for incandescent lamps.

3. The physical properties of HPS lamps

Extensive theoretical and experimental data on HPS lamps have been reported in other publications, and that information need not be reviewed extensively here. However, those properties that play a role in the stability of the spectral radiant flux produced by a lamp will be discussed to provide a foundation for an explanation of the measurements which were made.

3.1 Lamp construction

Because sodium vapor, operating at a high temperature, has a highly corrosive effect on ordinary glass or quartz, the high pressure sodium discharge was solely of theoretical interest for many years. The development of a translucent polycrystalline alumina (PCA) tube, resistant to sodium attack at high temperatures, and with high optical

transmittances in the visible range, made the HPS lamp technically feasible. Development of techniques for sealing sintered PCA ceramic tubes to carry electrodes and lead-in wires made it possible to actually manufacture such a lamp.

The heart of a conventional HPS lamp is a PCA tube filled with a sodium/mercury amalgam and an inert gas, usually xenon, used for starting the arc. A typical construction of a HPS lamp is illustrated in Fig. 1. The arc tube is mounted in an evacuated outer borosilicate glass bulb to isolate the tube from the ambient environment. The arc tube transmits >90% of visible radiation and can withstand the corrosive attack by hot sodium vapor. The PCA tube and outer glass envelope can withstand temperatures as high as 1600°C and 400°C, respectively. A getter material is used in the glass bulb to trap any impurities that may be released from the glass, arc tube and tube mounting structure. The diameter of the HPS arc tube is much smaller than that of mercury or metal halide lamps, and does not have a starting electrode inside the tube like other HID lamps. Therefore, the ballast for a HPS lamp contains a special starting circuit capable of ionizing the xenon gas, such as a low energy, high voltage pulse on each power line cycle or half cycle.
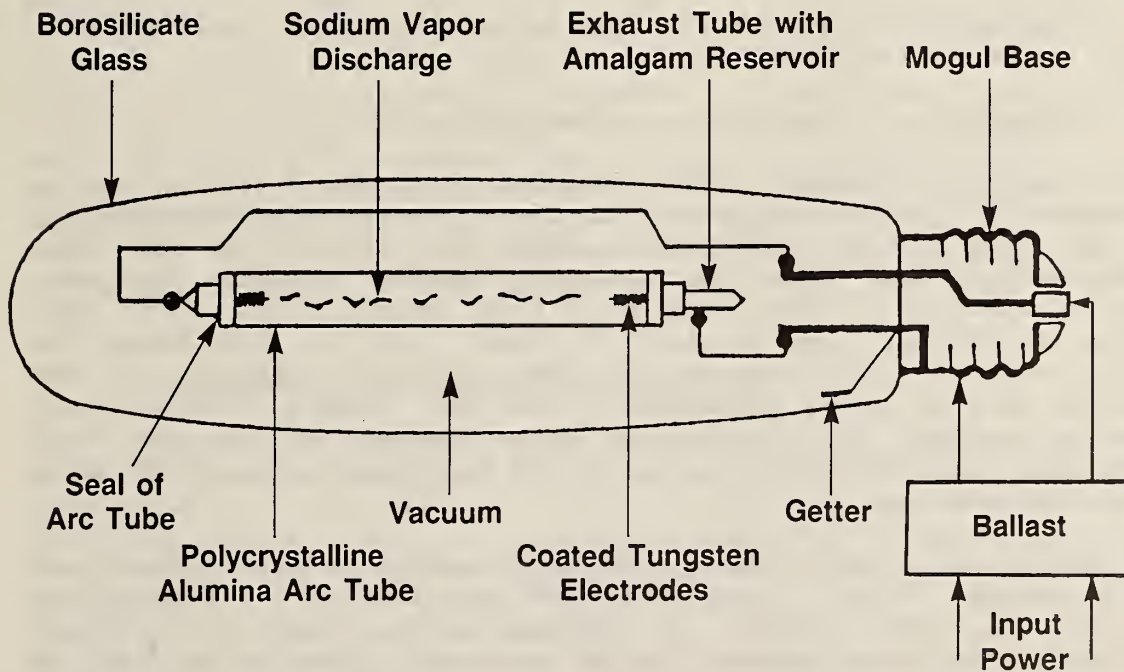

Fig 1. Typical construction of a High Pressure Sodium Discharge lamp.

3

3.2 Starting characteristics

When first started, the discharge is predominantly caused by the xenon gas. As the temperature starts to rise, and mercury vapor pressure builds up in the arc tube, more and more sodium is excited and the lamp color shifts from the bluish-white of ionized mercury and xenon to the yellow of sodium, and finally to golden-white produced by a large continuum spectrum in the red and green regions and a smaller amount in the blue and violet regions.

3.3 Design parameters and their effect on luminous efficacy and spectral distribution

The luminous efficacy of a HPS lamp depends upon the following design parameters:

(1) the sodium and mercury vapor pressures (which vary with the ratio of sodium to mercury, the amount and the operating temperature of the amalgam);

(2) the vapor pressure of the xenon;

(3) the discharge tube bore, length, wall thickness and tube materials;

(4) the tube wall loading (the lamp wattage divided by the effective surface area of the tube);

(5) the electrode construction and emitter materials.

An optimally designed 400W HPS lamp has the following design parameters [5]: the sodium, mercury and xenon pressures in the operating lamp are about 10^4 Pa, 8×10^4 Pa and 2×10^4 Pa, respectively; the inner diameter of the arc tube, the electrode spacing, and the tube wall thickness are about 7.5 mm, 82 mm and 0.6 mm, respectively; and the wall loading of the arc tube is about 20 W/cm^2, that is, just below the critical value for failure of the arc tube. The wall temperature of the discharge tube is mainly determined by the wall loading. The luminous efficacy increases with increasing tube diameter at constant wall temperature. A higher wall loading results in a higher luminous efficacy at constant diameter.

Like the metal halide lamps, HPS lamps contain an excess quantity of liquid amalgam, which is located behind the electrodes. During lamp operation, a small quantity of sodium/mercury amalgam is partially vaporized. The excess amalgam remains condensed in the coolest part of one end of the arc tube. The liquid amalgam can replenish any sodium lost from the arc discharge, thereby prolonging the life and somewhat stabilizing the electrical parameters of the HPS lamp.

The optical spectral power distribution of the HPS lamp is partly

determined by the vapor pressures of sodium and mercury, which are governed in turn by the ratio of sodium/mercury in the amalgam and the temperature of the coolest part of the arc tube. The color rendition and the luminous efficacy of an HPS lamp depend markedly on the shape of the spectrum in the region of the self-reversed sodium D-lines. A typical relative spectral power distribution curve is illustrated in Fig. 2 on the next page. The coolest part of the arc tube serves as a reservoir of the liquid amalgam which is kept at an optimum temperature for the desired characteristics of the lamp. The temperature of the amalgam may vary from approximately 600°C to 750°C, depending on the manufacturer. Some manufacturers place the amalgam reservoir external to the arc tube (see Fig. 1), but others use an inside corner of the tube. The partial vapor pressure of the sodium will depend upon the composition of the liquid phase at the operating temperature. If some radiation is reflected back to the reservoir, it will increase the temperature of the coolest part of the arc tube and then, the light output of the HPS lamp will change. If the amalgam temperature changes, the lamp voltage will change proportionately if not controlled. Therefore if stable flux is desired, the power supplied to the lamp must be well controlled by regularly adjusting the input voltage.

For a conventional HPS lamp, the ratio of sodium/mercury amalgam, the dimensions of the arc tube, the xenon pressure, and the wall loading are kept constant. However, the composition and the temperature of the amalgam will be changed by the normal blackening of the ends of the arc tube and/or the loss of sodium during lamp life. This will affect the stability of the light output of the lamp. If the sodium vapor pressure in an HPS lamp is increased by increasing the cool spot temperature, the separation of the intensity maxima on either side of the self-reversed D-lines, $\Delta\lambda$, (see Fig. 3) will be increased. If the sodium vapor pressure is increased with a corresponding decrease in mercury vapor pressure, the peaks of the spectral curve will be decreased asymmetrically. The maximum luminous efficacy is produced at a certain sodium/mercury ratio. For 400W HPS lamps, the mole fraction of sodium in amalgam is within the range of 0.625 - 0.76. The maximum efficacy is reached when a (25°C) sodium mole fraction of 0.70 is used at an amalgam temperature of 640°C [10].

3.3.1 Electric power dissipation mechanisms

All theoretical studies of the high pressure sodium vapor discharge are based on equating the input electric power to various power dissipation mechanisms [4,5,11]. For a 400W HPS lamp about 50 - 60 percent of the input power is transformed into radiant power, about 118W into the visible, about 80W into the infrared, and about 2W into the ultraviolet. About 5 percent of the input power is lost at the electrodes, and the rest is lost by heat-conduction [6, 12]. It is necessary to establish and solve the energy balance equation of the input-output process in order to predict the performance of arcs in high pressure sodium vapor.
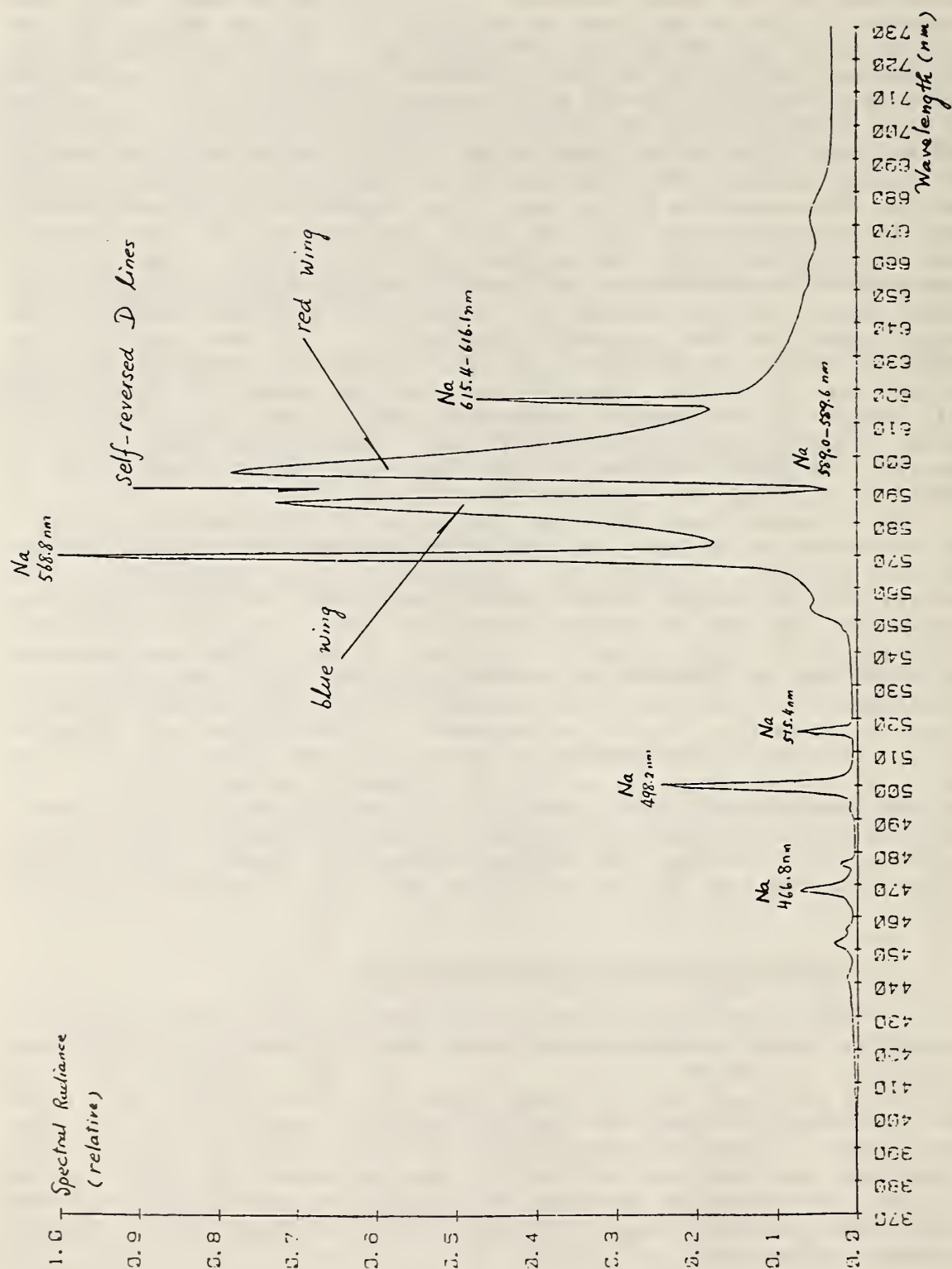
Fig 2. Optical spectral power distribution of a high pressure sodium
discharge lamp, relative radiance versus wavelength in nm.
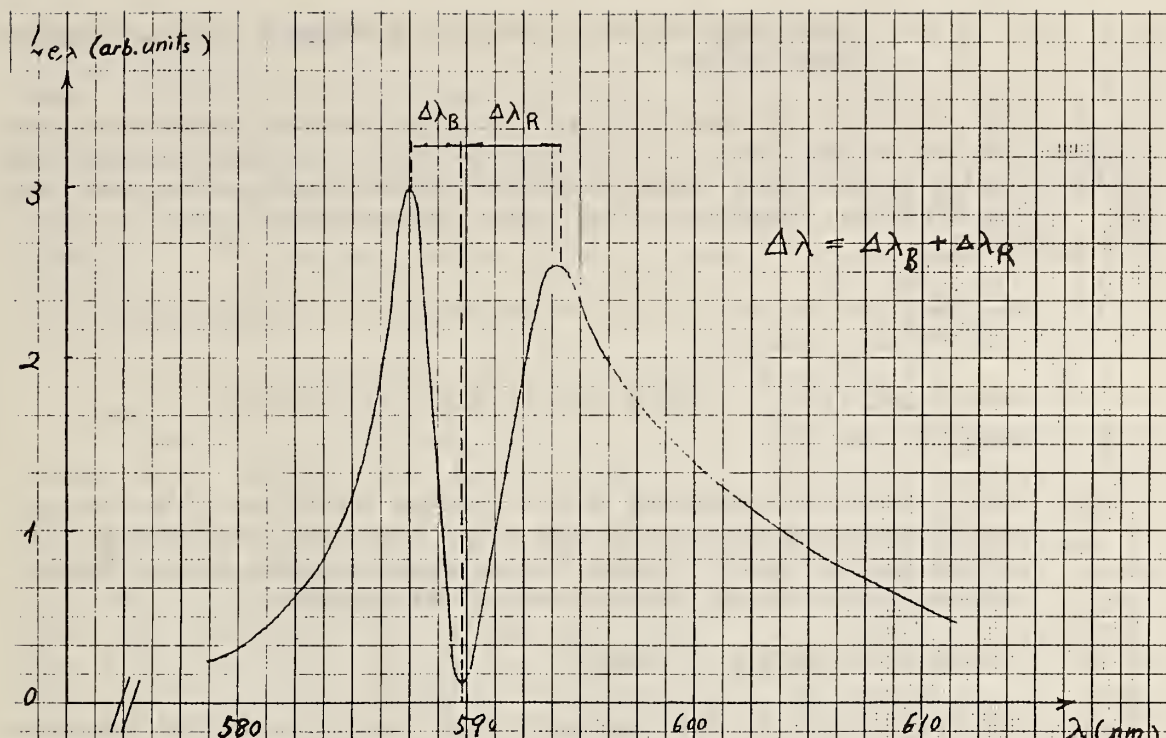
Fig 3. Expanded optical spectral power distribution of peaks in the region around the self reversed sodium D-lines, relative radiance versus wavelength in nm.

3.3.2 Optical spectrum parameters

3.3.2.1 Effects of the relative Hg and Na pressures

The broadening mechanisms of sodium D-lines include the resonance broadening due to the interactions between sodium atoms, and the Van der Waals broadening due to the sodium-mercury interactions. In a high pressure sodium discharge arc without mercury, the self-reversed profile of the D-lines is symmetrical and the width of the absorption depends on the sodium pressure. Because mercury atoms are present in the discharge tube of an HPS lamp, they influence the profile of D-lines and result in an asymmetrical line broadening (see Fig. 3). This asymmetrical broadening of the D-lines and the shift, $\Delta\lambda_R$, of the maximum of the red wing toward longer wavelengths is increased by increasing the mercury partial pressure [6,13].

7

3.3.2.2 Determination of partial pressures from spectral distribution

In order to estimate the existing sodium and mercury pressure during lamp operation, several researchers have both theoretically and experimentally studied the sodium resonance radiation from the HPS lamp. For a quantitative explanation of this asymmetrical profile, it is assumed that:

(1) the positive column in the arc discharge is a plasma with cylindrical symmetry;

(2) the plasma is in a steady state and near local thermodynamic equilibrium (LTE);

(3) the broadening mechanisms of the D-lines mainly include the resonance broadening due to the mutual interactions between the sodium atoms and the Van der Waals broadening due to the interactions between the sodium and mercury atoms;

(4) both D-lines interact strongly.

Thus, the relationship among $\Delta\lambda_B$, $\Delta\lambda_R$, and the partial pressure of sodium P_{Na} and mercury P_{Hg} are [14]:

$$\Delta\lambda_B = 2.23 \text{X} 10^{-5} \cdot P_{Na} \cdot R^{\frac{1}{2}} [\int_{-1}^{1} \frac{1}{T^2(\rho)} d\rho]^{\frac{1}{2}} - 3 \text{X} 10^{-8} \tag{1}$$

$$\Delta\lambda_R = \Delta\lambda_B + 4.78 \text{X} 10^{-8} \cdot P_{Na} \cdot P_{Hg} \cdot R(\Delta\lambda_R)^{\frac{1}{2}} \frac{\int_{-1}^{1} \frac{1}{T^2(\rho)} d\rho}{\Delta\lambda_B + \Delta\lambda_R} + 6 \text{X} 10^{-8} \tag{2}$$

Where $\Delta\lambda_B$ is the shift of the maximum of the blue wing from the center of the self-reversed D-lines;

$\Delta\lambda_R$ is the shift of the maximum of the red wing from the center of the self-reversed D-lines;

R is the radius of the arc tube;

$T(\rho)$ is the radial temperature distribution in the arc tube; and

ρ is the variable of radial distance from the central axis of the arc tube.

The function $T(\rho)$, with a strong radial gradient is roughly parabolic. Equation (1) indicates that the location of the maxima on the

blue side $\Delta\lambda_B$ depends only on the sodium vapor pressure P_{Na}. The shift of $\Delta\lambda_B$ provides a measure of the partial pressure of sodium in a burning lamp. From Eq. (2), the shift of the red wing maximum, $\Delta\lambda_R$ depends on both the sodium pressure P_{NA} and the mercury pressure P_{Hg}. As a result, the mercury partial pressure P_{Hg} can be determined by the difference between $\Delta\lambda_R$ and $\Delta\lambda_B$. The color appearance, color rendering and luminous efficacy of the HPS lamp are mainly determined by the sodium vapor pressure. The optimum sodium vapor pressure for maximum efficacy is achieved when the spacing $\Delta\lambda$ between the peaks of the blue and red wings is about 10 nm.

3.3.3 Role of mercury and xenon gases in the tube

Heat is carried from the arc to the tube wall primarily by the sodium vapor, because the thermal conductivity of sodium vapor is higher than that of xenon or mercury. The presence of the xenon and mercury vapors however, do serve to raise the vapor pressure and reduce the thermal conduction losses below that of the sodium alone, thereby improving the luminous efficacy of the lamp. In addition, the inert xenon gas starts the arc in the HPS lamps, and protects the electrodes from sodium corrosion during lamp ignition. The mercury vapor in the arc tube also has another important function during the lamp life. It serves to reduce the mobility of the electrons and thus increase the operating voltage of the HPS lamp to a more convenient value for matching the lamp to a ballast. On the other hand, the xenon and mercury atoms have higher excitation potentials than sodium, and their spectral lines therefore make a negligible contribution to the light output of the HPS lamp.

3.4 Design parameters' effects on life of lamp

Among all HID lamps, HPS lamps are the best in terms of stable lumen output. The total luminous flux of a 400W HPS lamp is about 98% of the initial value after operating for 17% of its lamp life (about 4,000 hrs.) and 73% at the end of its lamp life (about 24,000 hrs.).

The life of a HPS lamp depends primarily on the rate of rise of the lamp voltage during the lamp's life, and is dependent on the lamp wattage, ballast circuit, and design used by the manufacturer. According to one author, in most practical cases, the voltage rise is determined by a change in the sodium/mercury amalgam composition and temperature, with the loss of sodium from the tube playing a less important role [13]. The typical lamp starts its life operating at a voltage of about half the value of the line voltage. Eventually, the voltage rises so high that the power supplied by the ballast can no longer maintain the discharge, and the lamp will extinguish.

When selecting lamps for use as a standard, the rate of change in voltage across the lamp gives an indication of the future stability, and therefore the suitability of the lamp for use as a standard.

9

3.4.1 Temperature

The blackening of the inner wall of the arc tube by sputtered and evaporated electrode materials will raise the temperature of the amalgam, by raising the temperature of the coolest part of the tube which is situated near one of the electrodes. The increased temperature increases the sodium vapor pressure and lamp voltage.

The light output of HPS lamps will also be reduced by blackening around the electrodes. It should be mentioned also that, when the sintered PCA tube operates at a wall temperature above 1150°C, an excessive alumina sublimation rate could produce dark deposits on the vacuum outer glass bulb. If the thickness of deposits exceeds a value of about 10 nm, that can also cause significant radiant flux absorption.

3.4.2 Results of Na loss from tube

During the continuous operation of the HPS lamp, there is a slow loss of sodium from the arc tube which cannot be completely eliminated. The loss decreases the sodium/mercury ratio, thereby raising the mercury partial pressure which in turn increases the lamp voltage.

The loss of sodium from the tube is caused by several factors. Sodium can leak through the end seals of the arc tube, through the arc tube itself, or be lost by chemical combinations with other materials. The glasses used to seal the arc tube must be carefully selected to minimize the sodium leakage, and are usually composed of multicomponent oxides based on a $CaO-Al_2O_3$ system with additional additives. The quality of the seal is sensitive to small changes in manufacturing techniques. The sodium can also be lost by electrolysis through the tube wall and by chemically combining with sputtered or evaporated emitter materials, arc tube materials, sealing glass, or impurities. Sodium loss is accelerated if the HPS lamp is operated at excessive power [15].

4. Method of selecting stable lamps

To be a useful standard, a HPS lamp should have a dependable and known repeatability of light output on relighting, a long useful life, and electrical operating parameters that are within the normal values used by the customer, such as those specified by the American National Standards Institute (ANSI) [16]. The HPS lamps discussed in this paper have been chosen from the products of three U.S. manufacturers.

An initial process of selection and seasoning is described that ensured that the lamps were stable before calibrations are performed. Care had to be taken in the choice of a method used for evaluation of lamp changes with time. The luminous flux of the lamps of course could be compared between companies, but lamps produced by one company would change properties in a different way from lamps by a second company. For example, the relative spectral radiance as a function of wavelength changed with age on all lamps, but the pattern of the change in the relative spectrum differed from one manufacturer to another. Therefore,

10

some of the tests done on the lamps were valid only for comparison between lamps made by one manufacturer.

In order to select HPS lamps that will have a relighting repeatability of within ±1% of the mean value, close attention had to be paid to the changes in lamp output during seasoning. The suggested seasoning cycle consists of 1 hour off for every 11 hours burning time for a period of about 600 hours [17]. All lamps have been measured at a rated power of 400W. The power for seasoning the HPS lamp was supplied by an ELGAR Model 3001 AC voltage stabilizer. The recommendations of the CIE were followed, making measurements at intervals of about 100 hours to determine the changes in radiometric, photometric and electrical operating parameters as a function of time during the seasoning days [18].

The following evaluations of lamp performance were made:

(1) When operating inside an integrating sphere at 400 watts, the electrical parameters (lamp voltage V and lamp current I) were recorded. Relative values of the spectral radiance of the sphere window were measured, from which the integrated radiance L_e, luminance L_v, luminous flux Φ_v, chromaticity coordinates (x,y) and correlated color temperature T_c were calculated;

(2) Determination of $\Delta\lambda_R$ and $\Delta\lambda_B$ from the spectral power distribution curve; and

(3) Measurement of the relative intensity of one of the mercury spectral lines as a function of time during lamp ignition. After the arc in the HPS lamp has been stabilized, the mercury lines can no longer be detected. To determine clearly the transition time from mercury vapor discharge to sodium vapor discharge, the blue mercury line at 435.8 nm was chosen because the sodium continuum spectrum is weak at this wavelength.

All lamps were seasoned for 100 hours before luminous flux measurements were made. After this initial 100 hours of seasoning, flux measurements were made at approximately 100 hour intervals between 100 and 600 hours of operating time. From measurements made during this 500 hour period, it was found that lamps from certain manufacturers could be predicted to be stable if they met the following criteria: the light output varied by less than 2% per 100 hours of operation during the 100 to 600 hour burning period, the relative spectral power distribution changed negligibly, and the time for transition from mercury discharge to sodium discharge stayed constant. Meeting these criteria, these lamps could be expected to have a luminous flux stable to within 1% for an additional 500 hours. Such a lamp is suitable for use as a working standard. Typical data is given in Table II which will be discussed later. If the light output of an HPS lamp varies more than 2% per 100 hours of operation, irregular results could generally be expected, and this lamp should be rejected.

11

HPS lamps which had passed the stability screening test were turned off and on 10 times on different days to verify the repeatability of light output to within ±1% of the average value.

5. Description of the measurements

5.1 General

The nominal luminous fluxes of the high pressure sodium lamps were determined using the equipment shown schematically in Figure 4. The lamps were placed inside a 2 meter diameter integrating sphere, and readings of the luminous flux exiting the sphere were obtained with a commercial spectroradiometer with associated computer hardware and software. Similar readings were taken for incandescent lamps with known luminous fluxes, and then the luminous fluxes of the high pressure sodium lamps were obtained from the expression:

$$\Phi_{v,x} = \Phi_{v,s} \; S_{v,x}/S_{v,s} \qquad (3)$$

where $\Phi_{v,x}$ and $\Phi_{v,s}$ are the luminous fluxes of the test and standard lamps, and $S_{v,x}$ and $S_{v,s}$ are the photometric readings provided by the spectroradiometer and computer. The chart recorder was used for following changes in the intensity of spectral lines as a function of time. For more details on spectroradiometric measurements of luminous flux see references [19] and [20].
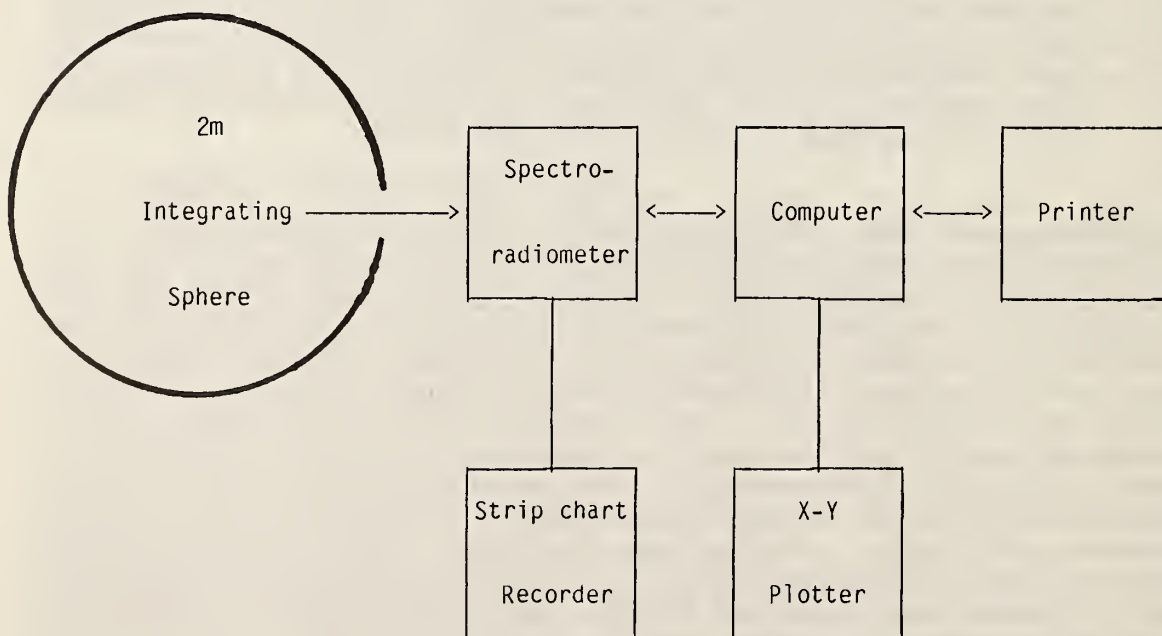
Fig 4. Schematic diagram of the experimental equipment.

12

5.2 Lamp operation

5.2.1 HPS lamps

The electrical circuit for electrical and photometric measurement of HPS lamps used is shown in Fig. 5. The AC power for HPS lamps was supplied by an ELGAR 3006B, 60Hz sine wave, line conditioner with harmonic distortion less than 0.2% and with regulation of ±0.025%. The voltage, current and wattage were measured by a YEW Type 2503 digital AC power meter with true rms response. One phase of the power supply and one side of the ammeter were grounded together in order to prevent the possibility of electrical shock.

The power to the HPS lamps passed through a reference ballast of the variable-impedance type. It consisted of an adjustable reactor and a variable resistor connected in series. The required values of impedance, power factor, and the corresponding current of the reference ballast were as specified by ANSI [21]. For a 400W HPS lamp, these values were:

Impedance: 38.6 ohm
Power factor: 0.075 ±0.005
Reference current: 4.6 amperes

Every time a change was made in the adjustment of the reference ballast, it was necessary to measure and to possibly reset the lamp voltage, current, and power factor.
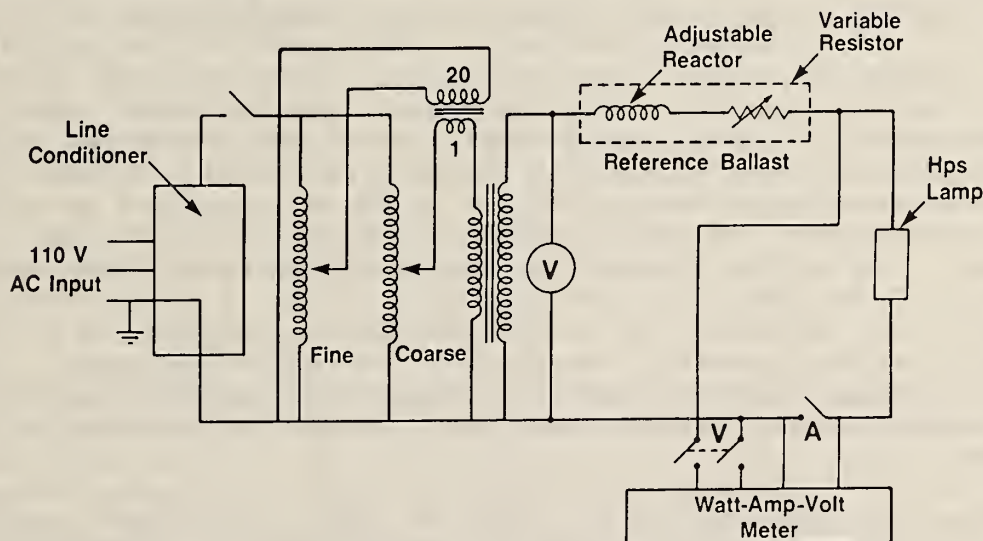
Fig 5. Electric circuit used for operation, control, and measurement of electrical parameters of HPS lamp.

Switches V and A were provided so that the voltmeter or ammeter impedance were removed from the circuit when not being used. The following electrical measurements were recorded: the voltage supplied to the lamp and ballast, the lamp current and the voltage across the lamp

13

with the lamp wattage held at 400W by adjusting the variable AC supply. Electrical characteristics of each HPS lamp were measured immediately after photometric measurements had been made.

The HPS lamps were operated for 40-60 minutes before making optical measurements so that the electrical characteristics and the light output would be stable. The HPS lamps were measured after the ambient temperature in the integrating sphere had been stabilized. (To shorten the testing period, the HPS lamps could be allowed to warm-up outside the sphere on an ordinary ballast, and then transferred to a reference ballast without being extinguished and moved into the sphere for measurement.)

5.2.2 Incandescent standards

A group of five 500-watt clear gas-filled incandescent lamps served as NBS working standards of total luminous flux and were used to obtain flux values for the HPS lamps. These incandescent lamps were run on DC power supplies, with a stability of 0.01%. The electrical parameters of the lamps were measured with a digital multimeter to an accuracy of 0.02%. The lamps were allowed to stabilize for at least 10 minutes before measurements were made.

5.3 Integrating sphere properties

The lamps were mounted vertically with the base up in the center of an integrating sphere. The inside of the integrating sphere was coated with pure barium sulfate powder, without binder to minimize absorption in the blue. A 7.6 cm diameter observation opening with a white diffusing plastic window was located on the sphere wall, from which the spectral radiance as a function of wavelength was measured using a spectroradiometer. A pear shaped baffle coated with commercial sphere paint shielded the sphere window from direct illumination by a lamp. The baffle screen was approximately 20.5 cm by 27 cm. For this work, the distance between the lamp and the baffle was about 1/3 of the radius of the sphere. The radiant flux of the lamp was diffusely reflected on the inner wall of the sphere and thus was depolarized. A blue filter was inserted between the window and the spectroradiometer in order to correct for the non uniform spectral throughput of the sphere photometer. The filter altered the relative spectral distribution of the flux incident on the spectroradiometer to approximate the distribution produced by the lamp alone.

Because the HPS lamp differs from the 500W incandescent standard lamp in self-absorption of luminous flux within the integrating sphere, the ratio of the self-absorption of the HPS lamp to that of the standard lamp was measured using a stable auxiliary incandescent lamp mounted near the inner wall of the integrating sphere. The auxiliary lamp had the same relative spectral power distribution as the standard lamp. No light from the auxiliary lamp could directly illuminate the observation window of the sphere, or the lamp in the test position. The unlighted standard lamp or the HPS lamp was located in turn at the center of the sphere.

14

The ratio of luminances of the observation window with the standard lamp in position to that with the HPS lamp in position, is the correction factor for self-absorption. Experimental results show this ratio, α, for three manufacturers' HPS lamps as follows:

Manufacturer	α
A	1.002
B	1.003
C	1.003

The corrected luminous flux of a HPS lamp is obtained by multiplying the measured flux by the ratio α.

The reflectance of the sphere used for the measurements has a slight spatial nonuniformity. Since the light leaving a HPS and incandescent lamp have different geometrical distribution patterns, it is possible that the measured signal is in error due to the combination of nonuniformities. In order to estimate the error due to this effect, sample lamps were measured in 4 positions differing by 45° in rotation about the vertical axis through the lamp. For each angle, the relative luminance on the observation window was measured by the spectroradiometer. The relative luminance differences of the standard lamp and the HPS lamp were less than 0.1% and much less than 0.1% respectively. No correction was made for this error. From previous experience, if the rotation interval were <45°, the estimated uncertainty due to a different spatial distribution would be less than 0.2%.

5.4 Spectroradiometer properties and measurement techniques

The spectral fluxes exiting from the sphere were measured using a Pritchard 1980B scanning spectroradiometer. The photomultiplier cathode of the spectroradiometer was illuminated for 40 minutes by power levels expected during later measurements. The output of the spectroradiometer varied as a function of time. A typical curve is illustrated in Figure 6. After the initial 40 minutes of exposure, the measurements were stable for an additional two and a half hours.

5.4.1 Linearity

The deviation from linear response of the detecting system depended chiefly on the level of the anode current of the photomultiplier in the spectroradiometer. The non-linearity was checked using the double-aperture method [22]. For our experimental conditions, the non-linearity of the reading for the spectroradiometer ranges of 10^{-2} and $10^{-3} WSr^{-1}m^{-2}nm^{-1}$ was 0.5% and 0.3% respectively. For the reading ranges from 10^{-4} to $10^{-7} WSr^{-1}m^{-2}nm^{-1}$, the non-linearity was negligible. No correction was applied to the data. If corrections for non linearity had been applied to the measured signals, the resulting corrected value of the luminous flux would have been about 0.2% higher than the flux based on uncorrected data.

15
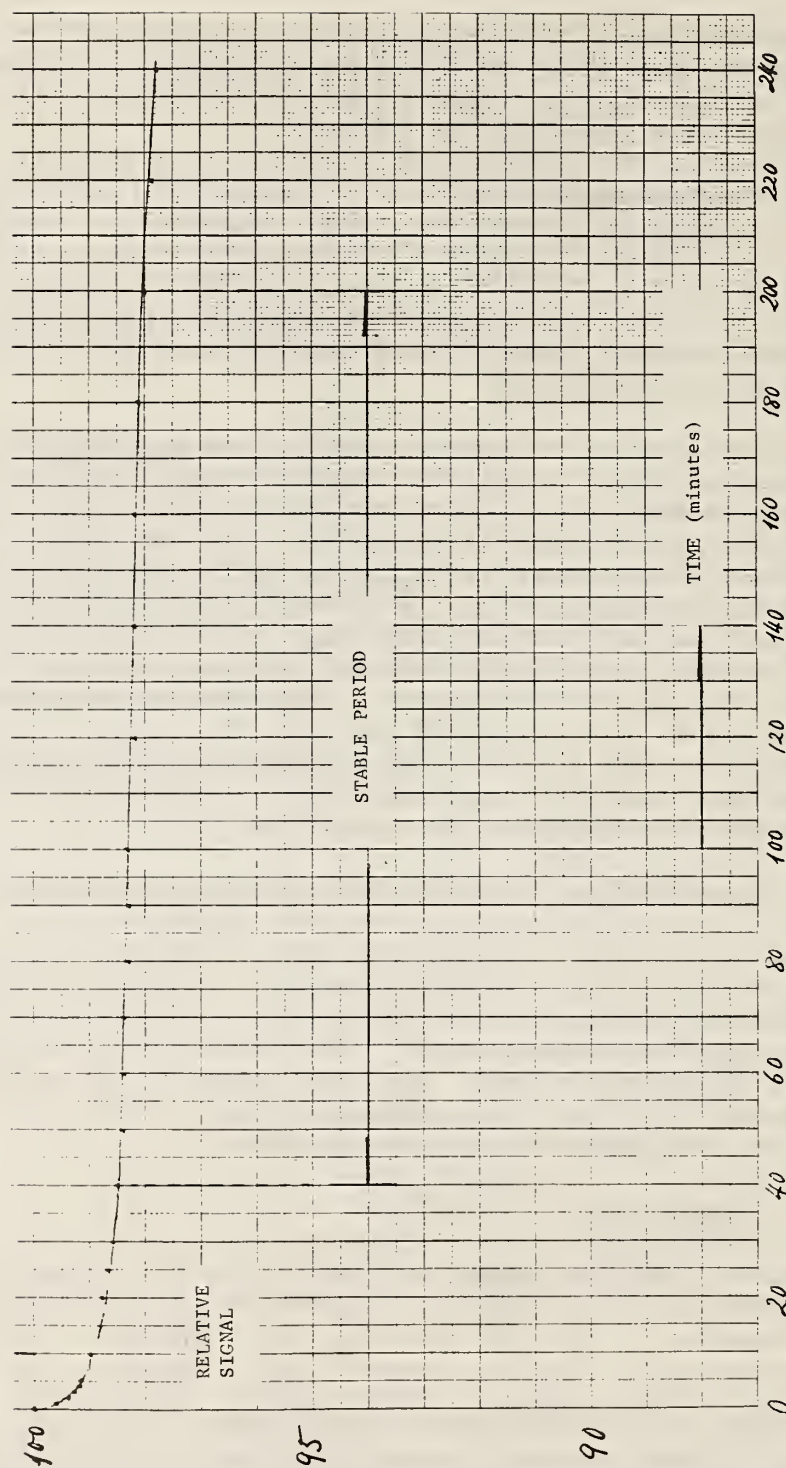
Fig 6. Signal from spectroradiometer as a function of time of exposure to a stable level of optical radiation.

5.4.2 Measuring aperture

The measuring field aperture of the spectroradiometer was chosen to be 20', 1°, or 3° for our experiments. Because the observation window in the sphere wall was a white diffusing plastic, and because it was illuminated by multiple diffuse reflections from the inner wall of the sphere, uniform luminance exited from the observation window. Experiments indicated that the different angular measuring fields did not affect the final value for total luminous flux. Since the total luminous flux of a 400W HPS lamp was higher than that of the 500W incandescent lamp, different field apertures were chosen for these two lamp types to match signal levels, and thereby avoid any possible non-linear response of the detecting system.

5.4.3 Wavelength range and interval

The spectral range covered 370 nm to 730 nm, using 1 nm, 5 nm or 10 nm bandpasses, and a wavelength sampling interval of 5 nm, the maximum suggested by CIE. Values for $V(\lambda)$ outside the measured region are <0.05% of the peak value, and therefore do not contribute significantly to the flux.

5.4.4 Wavelength scale accuracy

The spectroradiometer wavelength scale was checked by using the spectral lines of a low pressure mercury lamp in the visible range. The indicated readings of the digital wavelength scale were shifted toward longer wavelengths by 1 nm from the true value. Since an accurate measurement of the flux of these lamps will be later determined by goniometric measurements, a correction from the wavelength error was not made. It was estimated however, that such a correction would increase the values of the luminous flux by about 0.3%.

5.4.5 Spectral bandwidth

Spectral bandwidths of 10 nm, 5 nm or 1 nm were used during calibration of the HPS lamp. If the same bandwidth were chosen for measurements of both the HPS lamps and the standard lamp, the luminous flux assigned to a HPS lamp differed by only 0.1% to 0.2%, depending on bandwidth used. Thus, it is evident that the spectral power distribution of a HPS lamp can be measured by sampling as if it were a continuum spectrum. In order to reduce the measurement time to avoid possible long-term drift of the detecting system and to follow CIE suggestions, the band-width of 5 nm was chosen for measuring the luminous flux and the chromaticities of the lamps.

5.4.6 Radiometer AC response

The 500W working standards of total luminous flux were run on a DC power supply, but the HPS lamps were powered by an AC source. The luminous flux of the HPS lamp was therefore modulated at 120 hertz. The spectroradiometer was checked to see whether it responded to the varying

signal correctly.

The test showing insensitivity to an AC modulated signal used a chopped source, a rotating disk with two 90° apertures, inserted between a stable lamp and the spectroradiometer. The chopper was set at a rotational speed of 60 CPS, producing a chopping frequency of 120 Hz. The ratio of the readings with and without the chopper gave a measure of the transmittance of the chopper. In our experiment, the calculated transmittance of the sector disc was 0.5, based on measurements of the angular openings in the disc. For spectroradiometer reading ranges of 10^{-2} to 10^{-7} $WSr^{-1}m^{-2}nm^{-1}$, the relative difference between the calculated and measured transmittances was less than 0.1%. Therefore, the detecting system obeyed Talbot's Law.

5.5 Measurements made and analysis of the data

5.5.1 General description of spectroradiometer data acquisition

Under the measurement conditions described, the instrument photometric readings $S_{v,x}$ or $S_{v,s}$ appearing in Eq. (3) do not correspond precisely to the luminous fluxes of the test and standard lamps:

$$\Phi_v = K_m \int \Phi_\lambda\ V(\lambda)\ d\lambda \qquad (4)$$

where K_m = maximum luminous efficacy (lm/W), Φ_λ = spectral radiant flux, $V(\lambda)$ = values of spectral luminous efficiency for photopic vision. Rather, the readings are given by:

$$S_v = K_m \int \Phi_\lambda\ V(\lambda)\ f(\lambda)\ R(\lambda)\ d\lambda \qquad (5)$$

where $f(\lambda)$ is the spectral throughput of the integrating sphere and $R(\lambda)$ is the spectral responsivity of the spectroradiometer detection system.

Because the accuracy of calibration factors used by the data processing routines of the spectroradiometer were unknown, the following assumptions were made to estimate the magnitude of the systematic error that can result from the difference between the integrals of Eqs. (4) and (5):
   (1) The spectral distribution of a HPS lamp in a manufacturer's catalog represented the relative values of the HPS lamps' spectral distribution, $\Phi_{\lambda,x}$;
   (2) The spectral distribution of CIE Source "A" represented the relative values of the standard lamps' spectral distribution, $\Phi_{\lambda,s}$;
   (3) The throughput of the integrating sphere was estimated experimentally. The relative spectral irradiance of a lamp in one direction was measured on an optical bench using the Pritchard Spectroradiometer. The lamp was then operated in the

18

sphere used for calibrations. The spectral irradiance leaving the sphere was then measured with the same spectroradiometer. The ratios of the values of spectral irradiance were used as the values for $f(\lambda)$; and

(4) Values for instrument response $R(\lambda)$ were approximated by the relative response of a S-20 type photomultiplier.

The error in the measured luminous flux due to nonuniform sphere throughput was calculated by comparing the ratio of measured signals affected by the throughput of the sphere:

$$R_1 = \frac{\Sigma \ \Phi_{\lambda,x} \ V(\lambda) \ f(\lambda) \ d\lambda}{\Sigma \ \Phi_{\lambda,s} \ V(\lambda) \ f(\lambda) \ d\lambda}, \tag{6}$$

with the ratio of "true" signals that would be produced by a system with uniform throughput;

$$R_{True} = \frac{\Sigma \ \Phi_{\lambda,x} \ V(\lambda)d\lambda}{\Sigma \ \Phi_{\lambda,s} \ V(\lambda)d\lambda}. \tag{7}$$

The ratios calculated by these two different methods varied by +2.1%.

Similarly, the error in the measured luminous flux due to varying instrument response was calculated by comparing the ratio of measured signals that were affected only by the instrument response:

$$R_2 = \frac{\Sigma \ \Phi_{\lambda,x} \ V(\lambda) \ R(\lambda) \ d\lambda}{\Sigma \ \Phi_{\lambda,s} \ V(\lambda) \ R(\lambda) \ d\lambda} \tag{8}$$

with the ratio of "true" signals of Eq. (7). The ratios calculated by these methods differed by -3.7%.

Since the errors calculated by the above ratios are of opposite sign, the errors would cancel somewhat when combined in a ratio that is based on Eq. (5):

$$R_3 = \frac{\Sigma \ \Phi_{\lambda,x} \ V(\lambda) \ f(\lambda) \ R(\lambda) \ d\lambda}{\Sigma \ \Phi_{\lambda,s} \ V(\lambda) \ f(\lambda) \ R(\lambda) \ d\lambda} \tag{9}$$

When Eq. (9) is compared to the "true" value of Eq. (7) a net error of

-1.1% results. However since the assumptions used may not have applied, the errors calculated individually from the ratios R_1/R_{True} and R_2/R_{True} will be combined together in quadrature when determining the overall uncertainty of the measurements.

5.5.2 Summary of uncertainties evaluated

In addition to the errors associated with the HPS lamps and the equipment used in the measurements, there are error contributions due to the transfer from standards to test lamps, and to the standards themselves. The uncertainty of the working standards is taken from values in ref. [23]. Included are the total uncertainty of the working standards relative to the NBS primary reference group (1.1%), plus the random variation in the transfer from the working standards to the test lamps due only to the working standards (0.3%). (Since the HPS random variation was determined separately and is included in the 1.0% stability uncertainty, the random error of the standard is calculated as the square root of half of the square of the combined value reported in ref. [23].)

The possible sources of error and the estimated uncertainties in the spectroradiometric measurement of the luminous flux of HPS lamps are:

Item	Error Source	Uncertainty (%)
Spectroradiometer	Calibration factor	3.7
	Sphere throughput	2.1
	Wavelength error	0.3
	Non-linearity (residual error)	0.2
	Stability	0.2
HPS Lamp	Stability	1.0
	Self-absorption (residual error)	0.1
	Spatial distribution	0.2
	Digital wattmeter	0.3
Working Standards	Uncertainty relative to NBS standards	1.1
	Random variation of transfer	0.3
Total Uncertainty		±4.6%

(calculated from the square-root of the sum
of all uncertainties).

6.   Results of the measurements

6.1   Sphere measurements of total luminous flux

The measurements of lamp properties reported in this paper relied on measurements of luminous flux. For the determination of lamp stability and relighting repeatability, the flux did not have to be measured accurately. It was satisfactory to look at differences in uncorrected flux, as shown in Table II for stability over time, and similarly in Table V for repeatability. Corrections discussed in section 5 therefore

were not applied to the data in tables II through V. The tables are printed after the figures at the end of the text.

Luminous flux values for selected stable lamps appear in Table VI. The fluxes are based on the average of the relighting data in Table V, corrected only for lamp absorption in the sphere as discussed previously. The values of luminous flux are subject to the uncertainty discussed in the previous section.

6.2 Ambient temperature effects on luminous flux

The ambient temperature inside the integrating sphere during measurements was maintained at 35°C $\pm$ 5°C. In practice, it is difficult to maintain the ambient temperature at 25° $\pm$ 5°C as suggested by ref. [24]. The temperatures were measured using a copper-constantan thermocouple with a 0.1°C resolution digital-thermometer, positioned to the side at about the same height as the lamp, and shielded from the lamp. For a 400W HPS lamp, the temperatures at different positions inside the sphere are shown as follows:

d(cm)	8.0	16.5	26.0	36.5	50.5
t_o(°C)	36.9	35.4	36.4	37.2	37.2

where d is the distance between the thermocouple and the observation window, and t_o is the ambient temperature, which will vary with different lamps. The IES suggested position is at a distance between 20 cm to 1/3 of the sphere diameter from the inner wall [24].

As shown in Table I, the photometric characteristics of the HPS lamp depend very little on the ambient temperature after the sphere is closed for 5 minutes, and after 30 minutes the parameters are approximately constant.

6.3 Lamp wattage influence on luminous flux

The HPS lamp measurements during the stable operating period were made at different wattages to investigate the influence of lamp power on total luminous fluxes, radiant fluxes and chromaticities. The wattages were changed from 390W to 410W, Table III and Figs. 7 and 8 (on the next page) show that the luminous fluxes of the HPS lamp were proportional to the wattages between 396 and 408W. If the lamp wattage changed 1W at 400W, the luminous flux changed less than 0.4%, and the chromaticities remained the same. It was easy to control the wattage to within $\pm$ 0.25% of the rated 400W.

21
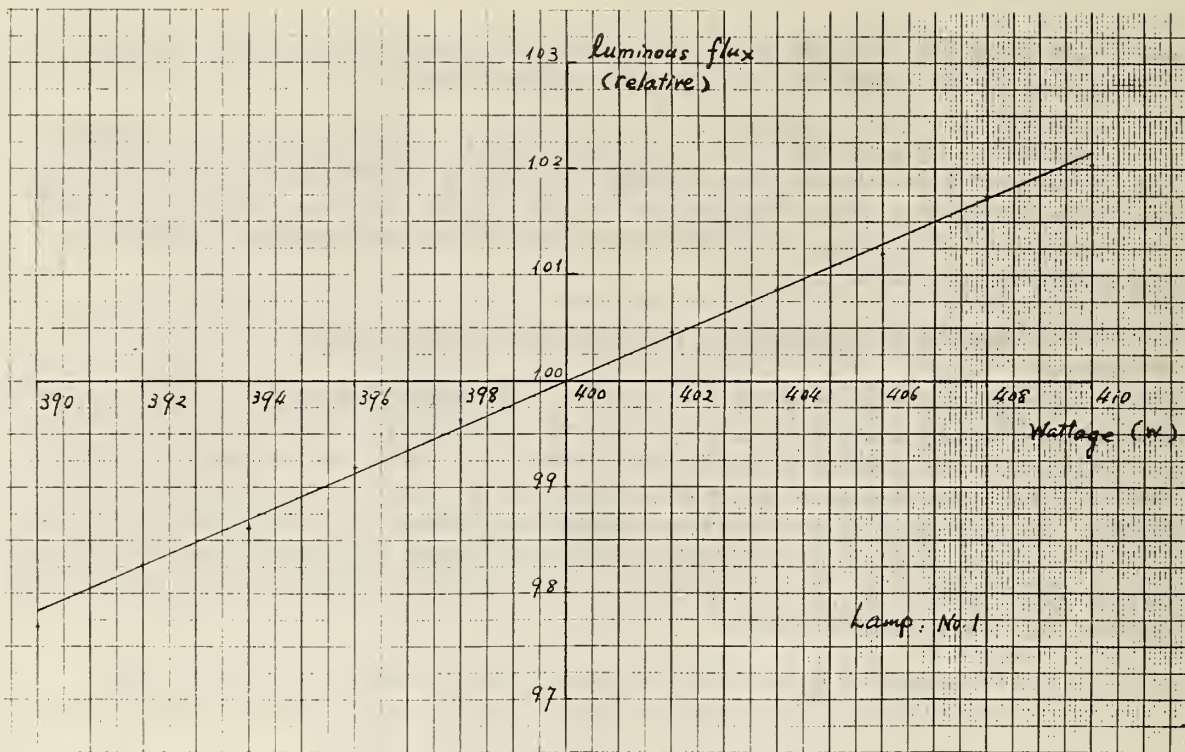
Fig 7.   Luminous flux of a HPS lamp from manufacturer A as a function of
          power through the lamp, relative radiance versus watts.
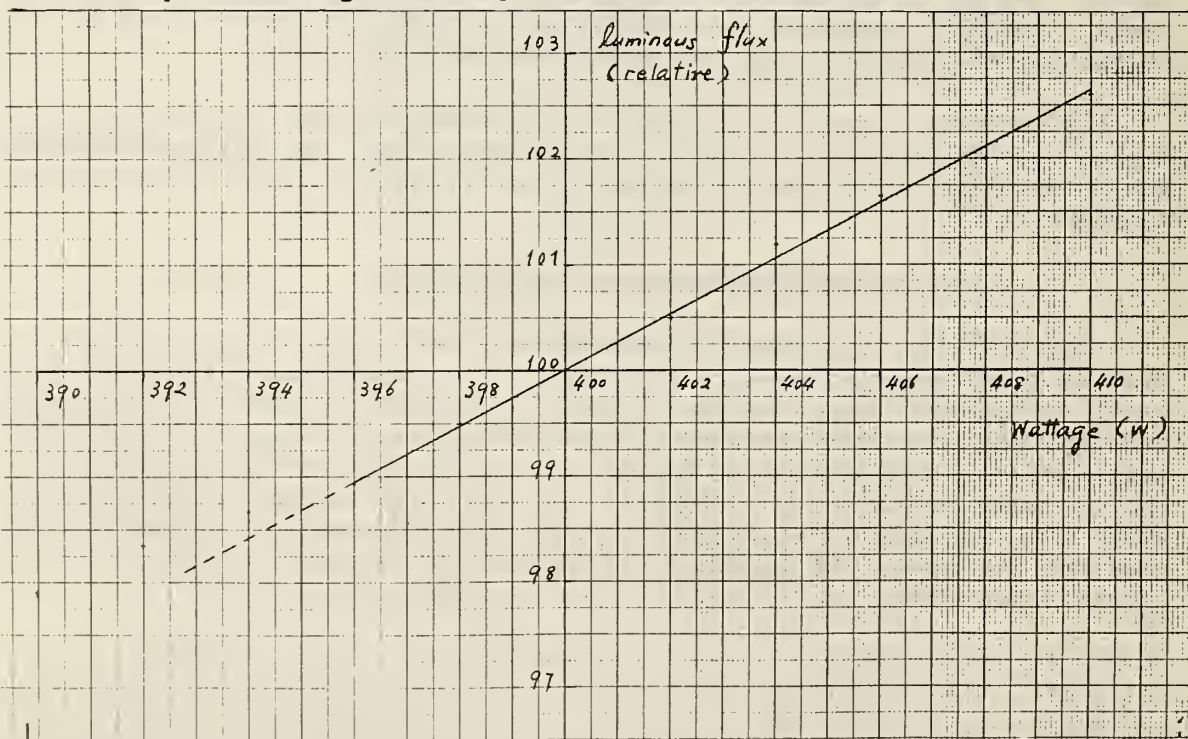
Fig 8.   Luminous flux of a HPS lamp from manufacturer B as a function of
          power through the lamp, relative radiance versus watts.

22

6.4 Repeatability of relighting

Changes in the amount of light produced by a lamp when relighted is of prime interest for lamps to be used as standards. Therefore a group of HPS lamps was tested for their repeatability of relighting.

After seasoning for about 500 hours, a group of HPS lamps was measured at least 10 times in two months, with no additional aging, operating the lamps only long enough to reach stability and to make readings. Each lamp was operated for a total of approximately 7 burning hours while conducting this test. The sphere signal from the HPS lamps was compared to the signal from the NBS working standards. The HPS lamps were found to repeat to within ±1.0%, satisfactory for use as a standard. The standard deviation of the repeated measurements of luminous flux of individual lamps ranged from 0.2% to 0.5%. The changes in radiant flux, lamp voltage, lamp current, correlated color temperature, and their relative standard deviations are shown in Table V.

6.5 Stability of lamps as a function of lamp burning time

6.5.1 Photometric

The data of Table II shows experimental results from measurements of a number of commercial 400W HPS lamps over a period of 1200 hours of operation. Among the lamps included in the table are lamps from 2 manufacturers, some found to be stable and others unstable. Measurements before approximately 500 hours, shown above the 1st dotted line, are burning times during which the lamps are being seasoned, and according to manufacturers' data would not be expected to be stable. After the 1st dotted line, and for an additional period of 400 to 600 hours of operation (depending on manufacturer), some lamps exhibited a "stable" period during which the relative luminous fluxes changed by less than ±1%. During that time, there was negligible visual increase of the end blackening of the arc tube. The second column under each lamp starts a new time for lamps considered to be in their stable period. After the second dotted line, the lamps had drifted in luminous flux by more than 1%, and were considered to have left the stable period of their life. These experiments were repeated with four more groups of lamps with similar results. A third manufacturer's lamps showed irregular results.

6.5.2 Spectral power distribution

The blue peak of the spectral power distribution depends only on sodium partial vapor pressure, while the red peak depends on both sodium and mercury vapor pressures. If the sodium/mercury ratio or the temperature of the amalgam changes during operation, the spacing of the peaks of the spectral distribution curve, $\Delta\lambda_B$ and/or $\Delta\lambda_R$ will shift indicating that the light output of the HPS lamp has been changed.

Experimental results are shown in Fig. 9 to 12. For two manufacturers' lamps, each lamp had the same profile during the time from

500 hours to about 1000 hours. After about 1000 hours, the blue and red peak profiles changed slightly. The widths of the blue peak and the red peak of one manufacturer's lamps showed some contraction (Fig. 9 and 10) and the others showed small expansion (Fig. 11 and 12). Accurate measurements of the wavelength shifts of $\Delta\lambda_B$ and $\Delta\lambda_R$ have been difficult because the burning time covered in our experiments was much shorter than the average life of the HPS lamp. But it was evident that the ratio of sodium/mercury amalgam and/or the temperature of the coolest part in the arc tube had changed slightly, and affected the luminous output of the HPS lamps. The third manufacturer's lamps showed irregular results. These results generally corresponded to the previous results shown in Table II.

6.5.3 Shift of discharge from mercury discharge to sodium discharge

During the HPS lamp ignition, the mercury vapor builds up and discharges in the arc tube. Then sodium vapor increasingly contributes to the light output. If the ratio of the sodium/mercury amalgam and/or the temperature of the coolest part changed slightly, the time to shift from mercury discharge to sodium discharge will change.

The signal at the blue mercury line, 435.8nm, was measured as a function of the ignition time when starting a HPS lamp. Typical curves are shown in Fig. 13 and 14. The signal due to the blue line increased to a maximum value in 50 to 80 seconds, then decreased to a minimum after 80 seconds to 130 seconds. The signal then rose again from the minimum, but this rise was due to the sodium discharge and not the mercury line. Finally, the signal approached a constant. The times varied with different lamps and at different periods in lamp life.

The experimental results for two manufacturers' lamps are tabulated in Table IV. The time the curve takes to reach a minimum is defined as the transition time from mercury discharge to sodium discharge. As the burning time is increased to 1000 hours or more, the transition time of one manufacturer's lamps increased slightly, while a second's lamps decreased. The third manufacturer's lamps show irregular results. These results also generally correspond to the results in Table II.

7. Summary

Fifty high pressure sodium lamps from 3 manufacturers have been extensively examined. Various properties of the lamps have been observed during 1200 hours of operation. From these measurements, those properties that are useful for predicting if a lamp will be stable, based on measurements made during lamp seasoning, have been determined. Twelve lamps have been selected that are predicted to have an estimated repeatability of light output within $\pm 1.0\%$, during an estimated useful life time of about 450 hours. These lamps are suitable for further spectral calibration. Their luminous flux has been measured. Further calibration will be done using a spectral goniometer.

Acknowledgment
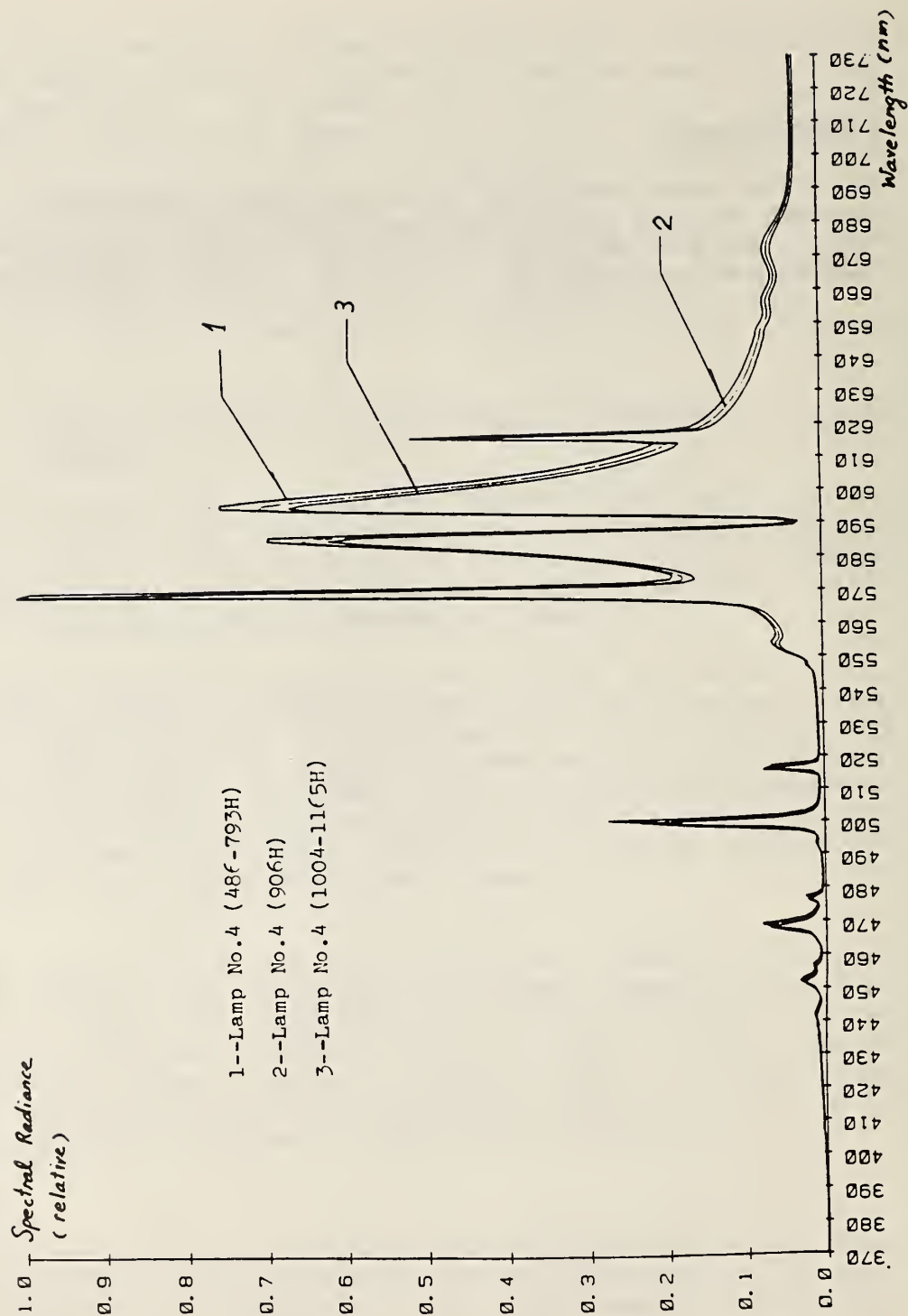
Fig 9. Spectral power distribution of a HPS lamp at various burning times. Curve 1 was the distribution measured at 486 hours of operation, 2 at 906 hours, and 3 at 1165 hours.
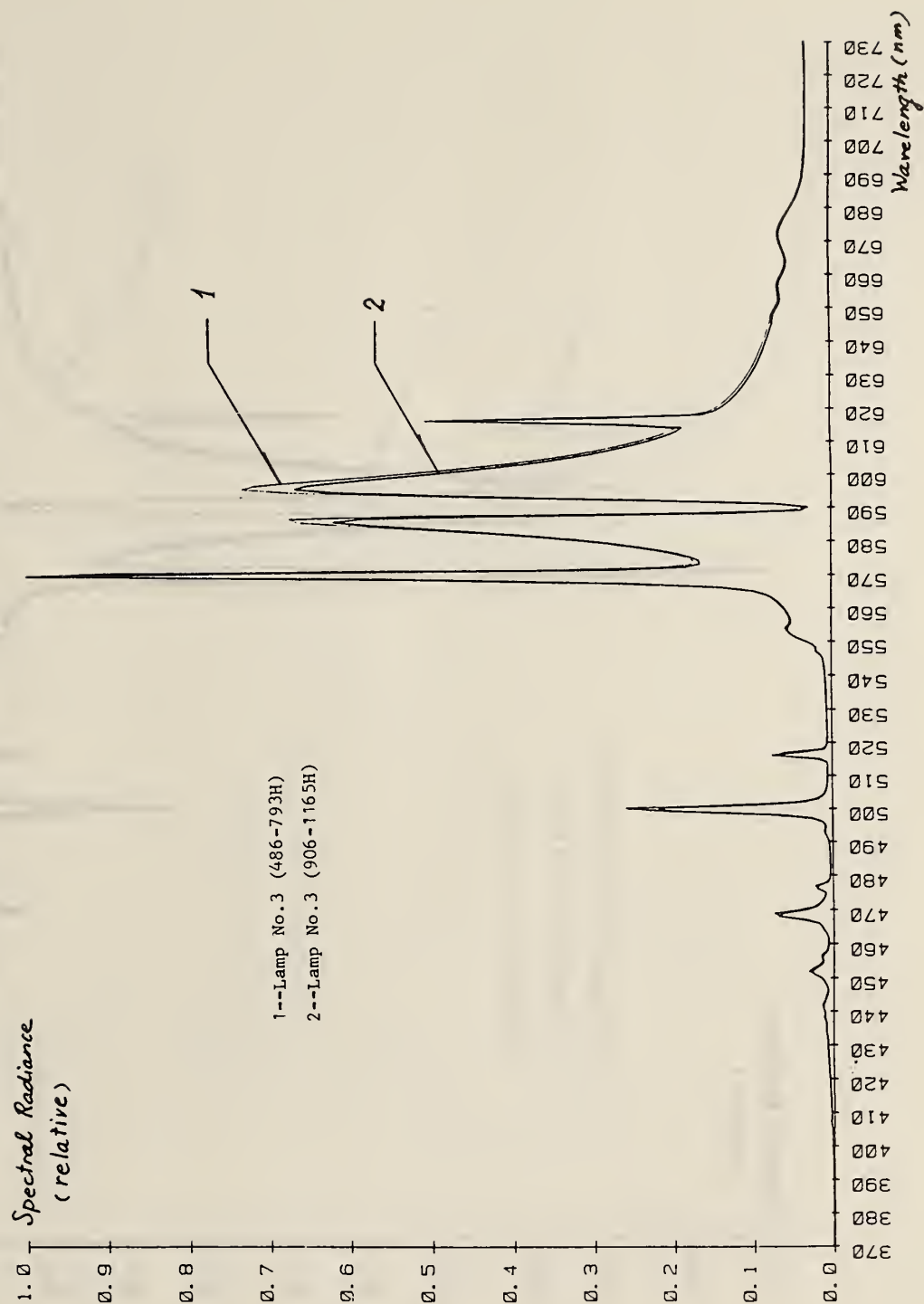
Fig 10. Spectral power distribution of a HPS lamp at various burning
times. Curve 1 was the distribution measured at 586 hours of
operation, curve 2 at 1095 hours.

27
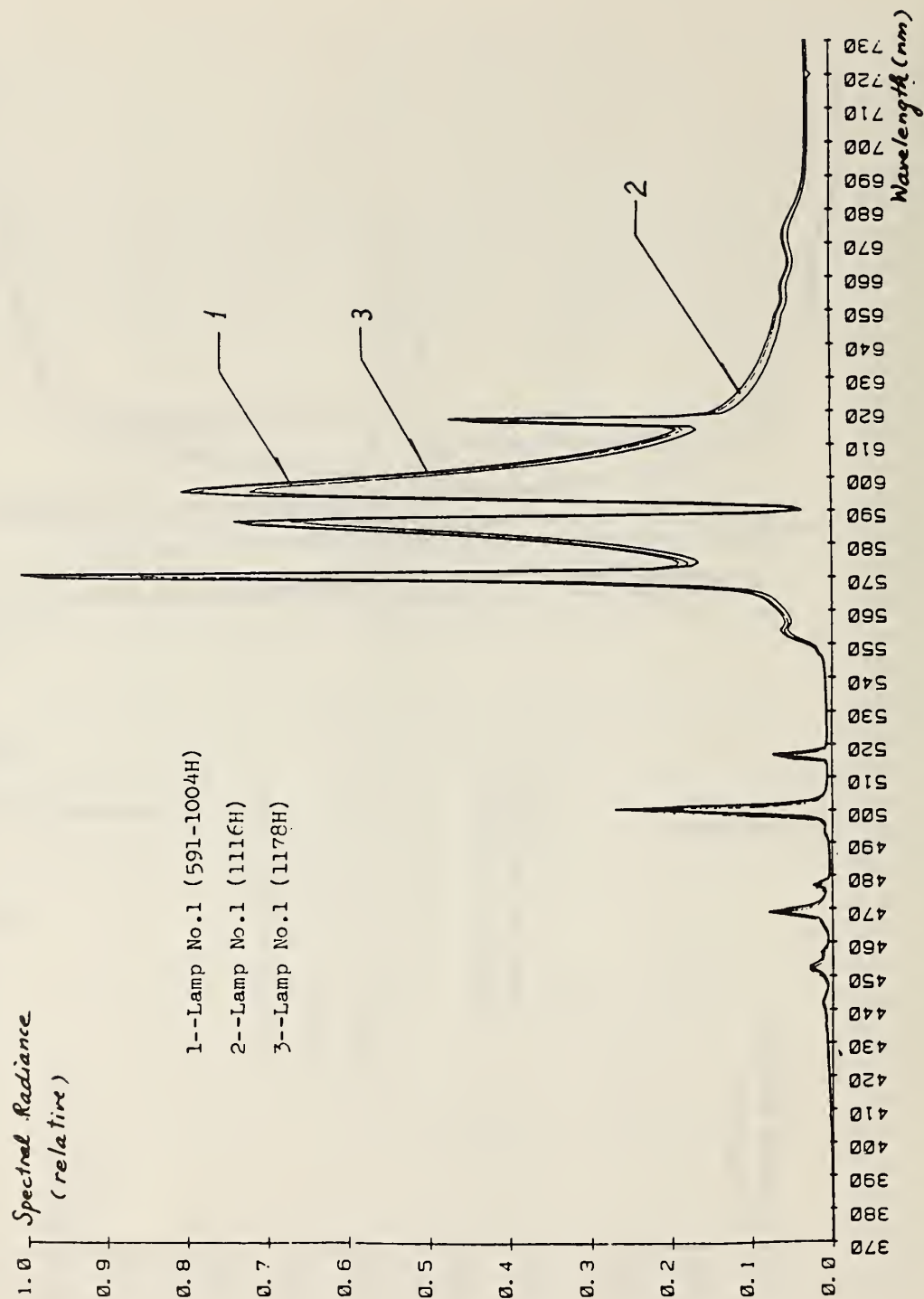
Fig 11. Spectral power distribution of a HPS lamp at various burning times. Curve 1 was the distribution measured at 591 hours of operation, 2 at 1116 hours, and 3 at 1178 hours.

28
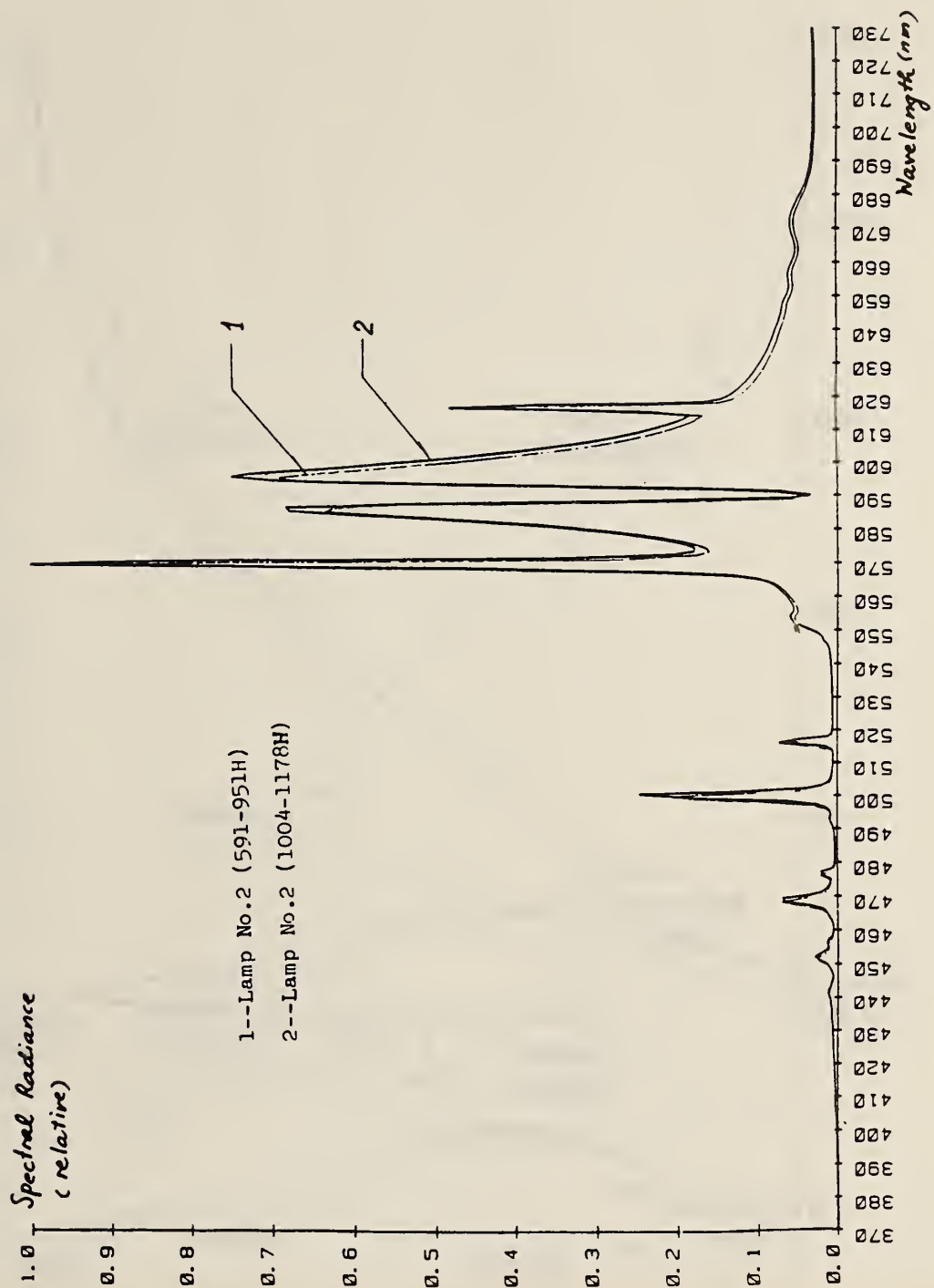
Fig 12. Spectral power distribution of a HPS lamp at various burning times. Curve 1 was the distribution measured at 748 hours of operation, curve 2 at 1116 hours.
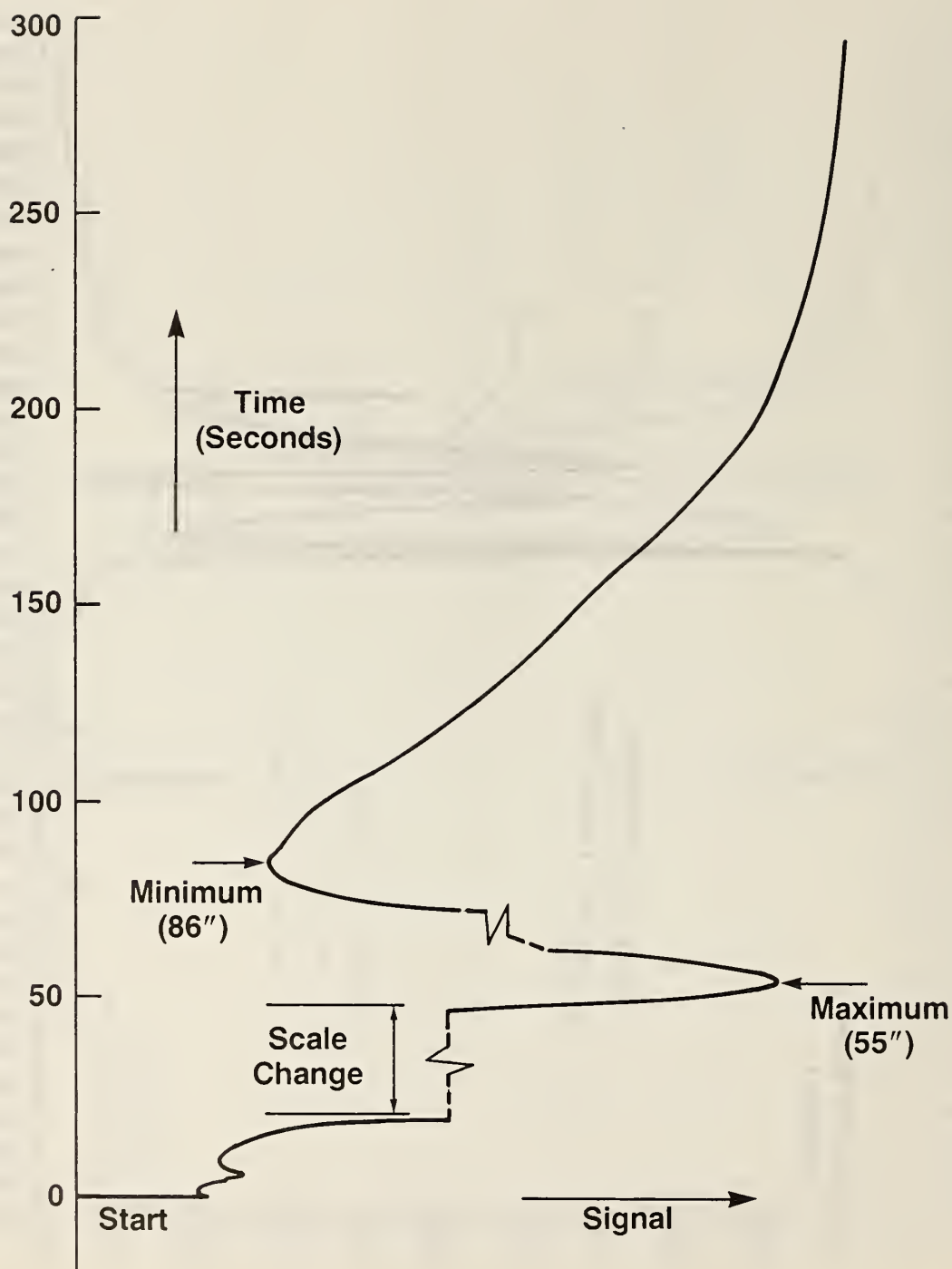
Fig 13. Relative spectral radiance of a HPS lamp measured at the 435.8nm mercury line as a function of time from lamp ignition. Relative radiance is plotted, with the signal amplification reduced between 22 and 48 seconds, against time in seconds. The sodium discharge matches the mercury discharge after 86 seconds of operation.
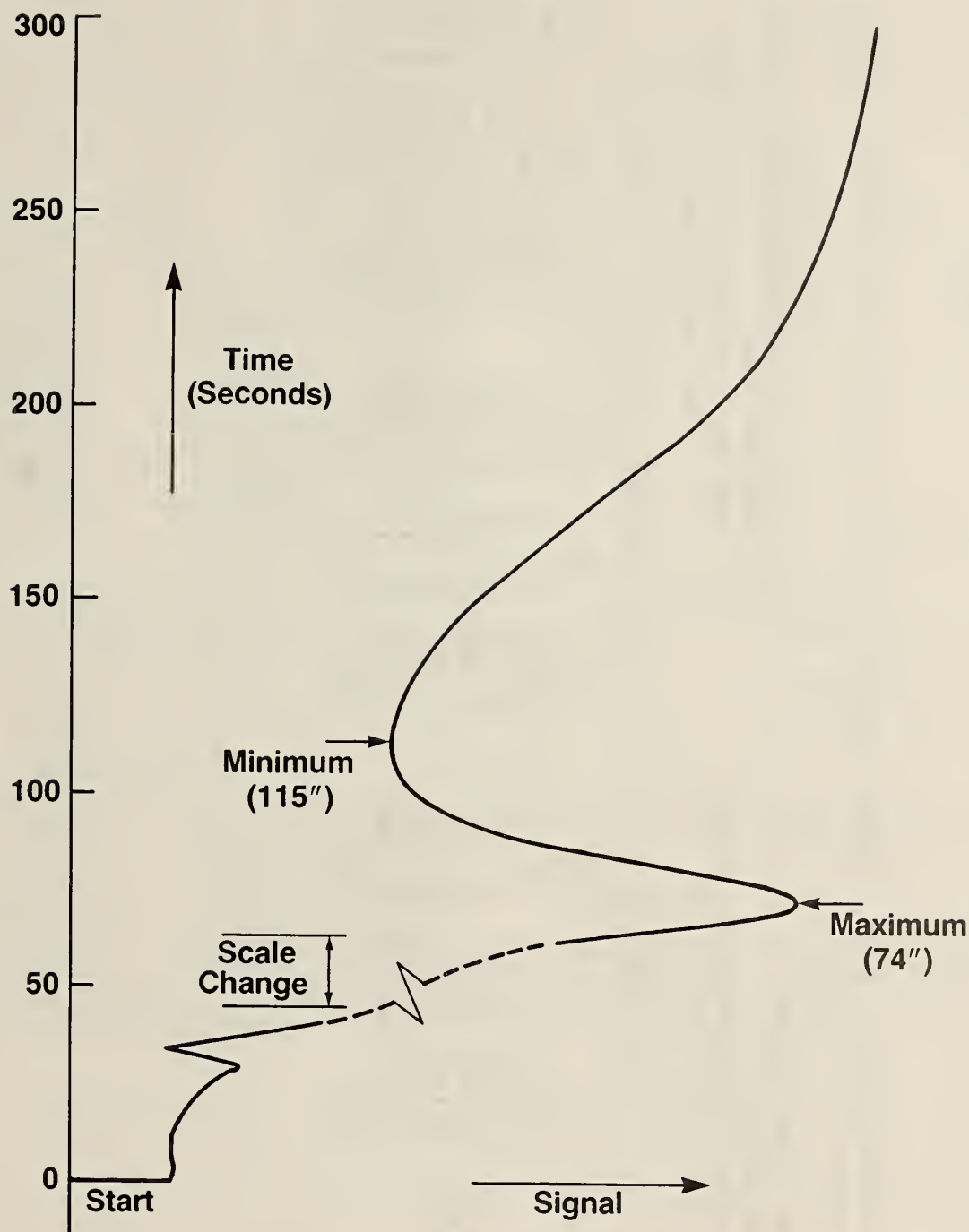
Fig 14. Relative spectral radiance of a HPS lamp measured at the 435.8nm mercury line as a function of time from lamp ignition. Relative radiance is plotted, with the signal amplification reduced at 50 seconds, against time in seconds. The sodium discharge has risen to match the mercury discharge, which is declining from its peak, after 115 seconds of operation.

Table I. Characteristics of HPS lamps operation over a one hour period after closing integrating sphere.

t : time after sphere is closed t_o: ambient temperature inside sphere
V : lamp voltage   I : lamp current
L_e: radiance on observation window L_v: luminance on observation window
x,y: chromaticity coordinates T_c: correlated color temperature

	HPS lamp (A)			HPS lamp (B)			HPS lamp (C)		
t (min)	5	30	70	5	30	60	5	30	60
t_o (°C)	31.1	34.5	34.7	30.9	34.3	34.2	29.9	33.8	34.2
V (V)	107.5	107.5	107.4	102.4	102.4	102.2	105.9	105.7	105.6
I (A)	4.370	4.366	4.372	4.521	4.520	4.528	4.435	4.444	4.446
L_e (x10 W/sr·m²)	2.346	2.345	2.342	2.268	2.273	2.274	2.260	2.255	2.258
L_v (x10³ cd/m²)	9.112	9.099	9.091	8.993	9.003	9.014	8.712	8.696	8.706
x	0.5218	0.5218	0.5219	0.5243	0.5243	0.5243	0.5221	0.5222	0.5222
y	0.4203	0.4203	0.4202	0.4147	0.4146	0.4147	0.4201	0.4201	0.4201
T_c (K)	2083	2083	2082	2028	2027	2027	2080	2078	2079

32

Table II. Luminous flux of HPS lamps as a function of operating life time.

Lamp No. 1

t_1 (hr)	t_2 (hr)	ϕ (lm)	$\frac{\Delta\phi}{\phi}$/100 hr	%
0		-		
162		50690		
262		50520	-0.34%	
377		50020	-0.86%	
477		50210	+0.38%	
591	0	49740	-0.94%	0
680	89	49350		-0.78%
748	157	49490		-0.50%
801	210	49520		-0.44%
851	260	49220		-1.00%
898	307	49380		-0.72%
951	360	49340		-0.80%
1004	413	49270		-0.95%
1054		49230		-1.02%
1116		49160		-1.16%
1178		49070		-1.34%

Lamp No. 2

t_1 (hr)	t_2 (hr)	ϕ (lm)	$\frac{\Delta\phi}{\phi}$/100 hr	%
0		-		
162		52210		
262		51960	-0.48%	
377		51510	-0.76%	
477		52190	+1.32%	
591	0	51230	-1.84%	0
680	89	51190		-0.08%
748	157	50810		-0.82%
801	210	51300		-0.14%
851	260	51240		+0.02%
898	307	51060		-0.33%
951	360	51210		-0.04%
1004	413	50900		-0.64%
1054	463	50790		-0.86%
1116		50510		-1.41%
1178		50450		-1.52%

Lamp No. 3

t_1 (hr)	t_2 (hr)	ϕ (lm)	$\frac{\Delta\phi}{\phi}$/100 hr	%
0	..	-		
162		50160		
262		49100	-2.11%	
377		49520	+0.75%	
477		48150	-2.77%	
591		48360	+0.44%	0
680		47650		-1.47%
748		48150		-0.43%
801		47590		-1.59%
		stop		

Lamp No. 4

t_1 (hr)	t_2 (hr)	ϕ (lm)	$\frac{\Delta\phi}{\phi}$/100 hr	%
0		-		
172		46580		
270		46440	-0.31%	
378		46950	+1.02%	
486	0	46590	+0.71%	0
586	100	46560		-0.06%
694	208	46560		-0.06%
793	307	46510		-0.17%
906	420	46530		-0.13%
1004	518	46370		-0.47%
1095	609	46370		-0.47%
1165	679	46180		-0.88%

Lamp No. 5

t_1 (hr)	t_2 (hr)	ϕ (lm)	$\frac{\Delta\phi}{\phi}$/100 hr	%
0		-		
172		46750		
270		46120	-1.38%	
378		46220	+0.20%	
486	0	45730	-0.98%	0
586	100	45770		+0.09%
694	208	45340		-0.85%
793	307	45720		-0.02%
906	420	45760		+0.07%
1004	518	45660		-0.15%
1095	609	45710		-0.04%
1165		45250		-1.05%

Remarks

t_1: operating time

t_2: operating time during stable period

ϕ: luminous flux

$(\Delta\phi/\phi)/100$: relative flux difference per 100 burning hours

%: relative flux difference from the beginning of the stable period

Table II. (Continued)

Lamp No. 6

t_1 (hr)	t_2 (hr)	Φ (lm)	$\frac{\Delta\Phi}{\Phi}$/100 hr	%
0		-		
172		47540		
270		46350	-2.55%	
378		46350	0	0
486		45260	-2.17%	-1.30%
586		44670		-0.54%
694		44430		-1.13%
793		43930		
		stop		

Lamp No. 7

t_1 (hr)	t_2 (hr)	Φ (lm)	$\frac{\Delta\Phi}{\Phi}$/100 hr	%
0		-		
100		50190		
232		49590	-0.91%	
345		48930	-1.18%	
491		49490	+0.78%	
500	0	48890		0
500		49390		+0.33%
500		49330		-0.04%
500		49070		-0.34%
500		49260		-0.83%
500	mean	49190		
628	128	49350		
736	236	49170		
834	334	49020		
951	451	48780		
1023	523	48520		-1.36%

Lamp No. 8

t_1 (hr)	t_2 (hr)	Φ (lm)	$\frac{\Delta\Phi}{\Phi}$/100 hr	%
0		-		
100		48650		
244		47920	-1.04%	
365		48050	+0.22%	
532		47560	-0.61%	
540	0	47760		0
540		47550		-0.08%
540		47390		-0.65%
540		47480		-0.57%
540		47750		-0.78%
540	mean	47590		
669	129	47550		
777	237	47280		
875	335	47320		
982	442	47220		
1054		46660		-1.95%

Lamp No. 9

t_1 (hr)	t_2 (hr)	Φ (lm)	$\frac{\Delta\Phi}{\Phi}$/100 hr	%
0		-		
110		47490		
228		46300	-2.13%	
388		46810	+0.69%	
486		45760	-2.29%	0
586		45660		-0.22%
702		45050		-1.55%
814		45160		+0.24%
		stop		

Lamp No. 10

t_1 (hr)	t_2 (hr)	Φ (lm)	$\frac{\Delta\Phi}{\Phi}$/100 hr	%
0		-		
110		47630		
228		47160	-0.84%	
388		45520	-2.17%	
486		45880	+0.81%	0
586		45170		-1.55%
702		45060		-1.78%
814		44540		-2.92%
		stop		

Remarks

t_1: operating time

t_2: operating time during stable period

Φ: luminous flux

$(\Delta\Phi/\Phi)/100$: relative flux difference per 100 burning hours

%: relative flux difference from the beginning of the stable period

34

Table III. Photometric and electrical properties of HPS lamps from two manufacturers as a function of power supplied to lamp.

W: Lamp Wattage

V: Lamp Voltage

I: Lamp Current

L_e: Percent of Integrated Radiant flux at 400 W

L_v: Percent of Luminous flux at 400 W

x,y: Chromaticity coordinates

T_c: Correlated color temperature

Lamp A

W(W)	V(V)	I(A)	L_e(%)	L_v(%)	x	y	T_c(K)
390	105.7	4.323	97.27	97.91	0.5242	0.4185	2051
392	106.2	4.329	97.90	98.35	0.5242	0.4185	2051
394	106.5	4.339	98.28	98.67	0.5241	0.4184	2052
396	106.8	4.348	98.61	98.94	0.5240	0.4185	2053
398	107.1	4.359	99.29	99.50	0.5240	0.4184	2053
400	107.4	4.368	100.0	100.0	0.5242	0.4183	2050
402	107.7	4.374	100.6	100.5	0.5241	0.4183	2051
404	108.1	4.383	101.5	101.2	0.5242	0.4182	2050
406	108.4	4.390	101.8	101.4	0.5241	0.4182	2051
408	108.8	4.397	102.5	102.0	0.5240	0.4182	2052
410	109.1	4.404	103.3	102.6	0.5241	0.4178	2048

Lamp B

W(W)	V(V)	I(A)	L_e(%)	L_v(%)	x	y	T_c(K)
390	101.6	4.486	96.60	97.69	0.5236	0.4167	2045
392	102.3	4.481	97.49	98.27	0.5240	0.4162	2039
394	102.8	4.480	98.10	98.63	0.5241	0.4160	2037
396	103.4	4.480	98.90	99.19	0.5240	0.4161	2038
398	103.9	4.481	99.43	99.63	0.5237	0.4162	2040
400	104.4	4.482	100.0	100.0	0.5236	0.4162	2041
402	105.0	4.484	100.5	100.5	0.5232	0.4164	2046
404	105.5	4.485	101.2	100.9	0.5233	0.4162	2044
406	106.0	4.484	101.7	101.2	0.5232	0.4162	2045
408	106.5	4.486	102.4	101.7	0.5231	0.4162	2046
410	107.0	4.486	102.8	102.0	0.5230	0.4164	2049

Table IV. "Transition time" for the radiation from sodium at 435.8 nm to rise and match the radiation from the mercury discharge.

t_1: Lamp operating time
t_2: Time in seconds from lamp start to minimum signal

Manufacturer A

t_1 (hr)	t_2 HPS lamp No. 1	t_2 HPS lamp No. 2	t_1 (hr)	t_2 HPS lamp No. 3	t_2 HPS lamp No. 4
898	87	87	500	89	91
951	88	87	610	88	92
1004	87	87	749	89	91
1054	85	87	861	88	93
1116	84	84	958	88	92
1178	80	79	1072	87	90
			1180	85	88

Manufacturer B

t_1 (hr)	t_2 HPS lamp No. 5	t_2 HPS lamp No. 6	t_1 (hr)	t_2 HPS lamp No. 7	t_2 HPS lamp No. 8
694	109	105	500	115	110
793	109	107	610	114	110
906	107	104	749	115	110
1004	107	108	861	115	110
1095	105	117	958	116	110
1165	122	122	1072	118	113
			1180	128	130

36

Table V. Repeatability of HPS lamp relighting.

ϕ_v: luminous flux, ϕ_e: radiant flux (relative),

%: relative difference from mean
σ: standard deviation
σ_0: fractional standard deviation

Date	Lamp No. 1S ϕ_v(lm)	%	ϕ_e	%	Lamp No. 2S ϕ_v(lm)	%	ϕ_e	%	Lamp No. 3S ϕ_v(lm)	%	ϕ_e	%
3/3-3/5	51310	-0.14	3.431	-0.26	48830	-0.77	3.181	-0.38	50630	-0.55	3.285	+0.06
3/21	50910	-0.91	3.406	-0.99	49030	-0.37	3.181	-0.38	50860	-0.10	3.289	+0.18
4/2-4/3	51410	+0.06	3.463	+0.67	49230	+0.04	3.181	-0.38	50980	+0.14	3.276	-0.21
4/8-4/9	51480	+0.19	3.429	-0.32	49250	+0.08	3.176	-0.53	51080	+0.33	3.294	+0.34
4/28	51430	+0.10	3.436	-0.12	49470	+0.53	3.221	+0.88	51000	+0.18	3.257	-0.79
5/5-5/6	51470	+0.18	3.433	-0.20	49360	+0.30	3.200	+0.22	51060	+0.29	3.289	+0.18
6/9	51620	+0.47	3.449	+0.26	49230	+0.04	3.188	-0.16	50960	+0.10	3.283	0
6/16	51130	-0.49	3.435	-0.15	49070	-0.28	3.199	+0.19	50770	-0.28	3.287	+0.12
6/19-6/23	51380	0	3.461	+0.61	49180	-0.06	3.210	+0.53	50920	+0.02	3.302	+0.58
6/25-6/26	51630	+0.49	3.455	+0.44	49400	+0.39	3.196	+0.09	50820	-0.18	3.272	-0.34
mean	51380		3.440		49210		3.193		50910		3.283	
σ	218.5		0.0174		190.2		0.0146		139.7		0.0126	
σ_0	4.25×10^{-3}		5.06×10^{-3}		3.87×10^{-3}		4.56×10^{-3}		2.74×10^{-3}		3.82×10^{-3}	

Date	Lamp No. 4S ϕ_v(lm)	%	ϕ_e	%	Lamp No. 5S ϕ_v(lm)	%	ϕ_e	%	Lamp No. 6S ϕ_v(lm)	%	ϕ_e	%
3/3-3/5	50090	-0.44	3.282	-0.12	51130	-0.53	3.333	-0.60	51370	-0.35	3.362	-0.33
3/21	50200	-0.22	3.283	-0.09	51270	-0.25	3.346	-0.21	51420	-0.25	3.374	+0.03
4/2-4/3	50220	-0.18	3.289	+0.09	51660	+0.51	3.369	+0.48	51690	+0.27	3.368	-0.15
4/8-4/9	50470	+0.32	3.276	-0.30	51490	+0.18	3.339	-0.42	51580	+0.06	3.387	+0.42
4/28	50320	+0.02	3.286	0	51480	+0.16	3.370	+0.51	51750	+0.39	3.364	-0.27
5/5-5/6	50330	+0.04	3.298	+0.37	51470	+0.14	3.345	-0.24	51620	+0.14	3.380	+0.21
6/9	50480	+0.34	3.289	+0.09	51470	+0.14	3.350	-0.09	51580	+0.06	3.367	-0.18
6/16	50400	+0.18	3.278	-0.24	51230	-0.33	3.357	+0.12	51380	-0.33	3.366	-0.21
6/19-6/23	50250	-0.12	3.286	0	51380	-0.04	3.369	+0.48	51580	+0.06	3.378	+0.15
6/25-6/26	50380	+0.14	3.290	+0.12	51430	+0.06	3.354	+0.03	51530	-0.04	3.382	+0.27
mean	50310		3.286		51400		3.353		51550		3.373	
σ	124.7		6.38×10^{-3}		153.4		0.0131		127.3		8.59×10^{-3}	
σ_0	2.48×10^{-3}		1.94×10^{-3}		2.99×10^{-3}		3.90×10^{-3}		2.47×10^{-3}		2.55×10^{-3}	

37

Table V. (Continued)

Date	Lamp No. 7S				Lamp No. 8S				Lamp No. 9S			
	Φ_v(lm)	%	Φ_e	%	Φ_v(lm)	%	Φ_e	% .	Φ_v(lm)	%	Φ_e	%
1/31	49730	+0.10	3.413	+0.26	50230	-0.20	3.430	+0.03	49840	-0.76	3.482	+0.66
3/3	49630	-0.10	3.401	-0.09	50390	+0.12	3.441	+0.35	50130	-0.18	3.441	-0.29
3/24-3/25	49690	+0.02	3.403	-0.03	50310	-0.04	3.435	+0.18	50300	+0.16	3.459	0
4/21-4/25	49800	+0.24	3.412	+0.24	50350	+0.04	3.427	-0.06	50490	+0.54	3.465	+0.17
5/2	49470	-0.42	3.391	-0.38	50120	-0.42	3.399	-0.82	50270	+0.10	3.436	-0.66
5/5-5/6	49750	+0.14	3.387	-0.50	50550	+0.44	3.436	+0.20	50040	-0.36	3.448	-0.32
6/10	49700	+0.04	3.405	+0.03	50360	+0.06	3.425	-0.12	50310	+0.18	3.466	+0.20
6/17	49780	+0.20	3.407	+0.09	50360	+0.06	3.425	-0.12	50310	+0.18	3.462	+0.09
6/20	49530	-0.30	3.404	0	50220	-0.22	3.429	0	50300	+0.16	3.459	0
6/24-6/25	49670	-0.02	3.417	+0.38	50390	+0.12	3.444	+0.44	50250	+0.06	3.468	+0.26
mean	49680		3.404		50330		3.429		50220		3.459	
σ	106.0		9.38×10^{-3}		117.5		0.0124		179.5		0.0136	
σ_0	2.13×10^{-3}		2.76×10^{-3}		2.34×10^{-3}		3.63×10^{-3}		3.57×10^{-3}		3.95×10^{-3}	

Date	Lamp No. 10S				Lamp No. 11S				Lamp No. 12S			
	Φ_v(lm)	%	Φ_e	%	Φ_v(lm)	%	Φ_e	%	Φ_v(lm)	%	Φ_e	%
1/31	49730	-0.46	3.370	-0.85	48970	+0.14	3.317	-0.42	47520	-0.19	3.314	+0.36
3/3	49780	-0.36	3.377	-0.65	48930	+0.06	3.349	+0.54	47850	+0.50	3.297	-0.15
3/24-3/25	50010	+0.10	3.380	-0.56	48730	-0.35	3.312	-0.57	47670	+0.13	3.307	+0.15
4/21-4/25	50250	+0.58	3.422	+0.68	49130	+0.47	3.342	+0.33	47350	-0.55	3.272	-0.91
5/2	50140	+0.36	3.399	0	49010	+0.22	3.332	+0.03	47540	-0.15	3.291	-0.33
5/5-5/6	49740	-0.44	3.385	-0.41	48930	+0.06	3.316	-0.45	47600	-0.02	3.309	+0.21
6/10	50090	+0.26	3.415	+0.47	48710	-0.39	3.312	-0.57	47690	+0.17	3.313	+0.33
6/17	49980	+0.04	3.413	+0.41	48930	+0.06	3.350	+0.57	47450	-0.34	3.290	-0.36
6/20	49980	+0.04	3.414	+0.44	48780	-0.25	3.335	+0.12	47780	+0.36	3.312	+0.30
6/24-6/25	49850	-0.22	3.412	+0.38	48870	-0.06	3.342	+0.33	47680	+0.15	3.310	+0.24
mean	49960		3.399		48900		3.331		47610		3.302	
σ	177.1		0.0190		130.3		0.0152		153.1		0.0137	
σ_0	3.54×10^{-3}		5.60×10^{-3}		2.67×10^{-3}		4.56×10^{-3}		3.22×10^{-3}		4.15×10^{-3}	

Table V. (Continued)

V: lamp voltage, T_c: correlated color temperature
A: lamp current,   %: relative difference from mean

Lamp No. 1S					Lamp No. 2S				
V(V)	%	I(A)	%	T_c(K)	V(V)	%	I(A)	%	T_c(K)
98.8	-0.60	4.704	+0.38	2057	92.4	+0.11	4.972	-0.40	2066
99.5	+0.10	4.674	-0.26	2083	91.8	-0.54	5.015	+0.46	2090
100.1	+0.70	4.657	-0.61	2023	92.0	-0.33	5.002	+0.20	2081
98.7	-0.70	4.709	+0.49	2074	92.3	0	4.989	-0.06	2094
98.7	-0.70	4.711	+0.53	2062	92.3	0	4.997	+0.10	2051
98.6	-0.80	4.719	+0.70	2084	92.1	-0.22	5.007	+0.30	2091
99.4	0	4.693	+0.15	2095	92.2	-0.11	5.006	+0.28	2100
100.1	+0.70	4.654	-0.68	2110	93.0	+0.76	4.965	-0.54	2110
99.8	+0 40	4.672	-0.30	2089	92.6	+0.33	4.978	-0.28	2093
99.9	+0.50	4.664	-0.47	2077	92.5	+0.22	4.985	-0.14	2087
99.4		4.686		2075	92.3		4.992		2086
0.611		0.0243		24.0	0.318		0.0165		16.9
6.15×10^{-3}		5.18×10^{-3}		1.15×10^{-2}	3.45×10^{-3}		3.31×10^{-3}		8.11×10^{-3}

Lamp No. 3S					Lamp No. 4S				
V(V)	%	I(A)	%	T_c(K)	V(V)	%	I(A)	%	T_c(K)
92.9	+0.65	4.955	-0.78	2063	94.0	+0.11	4.900	-0.26	2057
92.0	-0.33	5.006	+0.24	2078	93.6	-0.32	4.929	+0.32	2083
92.2	-0.11	4.998	+0.08	2084	95.8	+2.02	4.819	-1.91	2067
91.8	-0.54	5.015	+0.42	2061	94.1	+0.21	4.902	-0.22	2084
91.8	-0.54	5.016	+0.44	2082	93.7	-0.21	4.922	-0.18	2053
91.8	-0.54	5.020	+0.52	2089	93.5	-0.43	4.929	+0.33	2033
92.4	+0.11	4.995	+0.02	2102	93.8	-0.11	4.927	+0.29	2080
92.6	+0.33	4.985	-0.18	2097	93.7	-0.21	4.929	+0.33	2095
92.7	+0.43	4.976	-0.36	2095	93.7	-0.21	4.930	+0.35	2088
92.7	+0.43	4.978	-0.32	2087	93.4	-0.53	4.940	+0.55	2090
92.3		4.994		2084	93.9		4.913		2072
0.425		0.0209		13.6	0.690		0.0353		19.6
4.61×10^{-3}		4.19×10^{-3}		6.51×10^{-3}	7.34×10^{-3}		7.18×10^{-3}		9.47×10^{-3}

39

Table V. (Continued)

Lamp No. 5S					Lamp No. 6S				
V(V)	%	I(A)	%	T_c(K)	V(V)	%	I(A)	%	T_c(K)
93.3	-0.74	4.935	+0.49	2065	94.3	+0.11	4.894	-0.18	2073
93.4	-0.64	4.933	+0.45	2072	94.3	+0.11	4.894	-0.18	2078
93.9	-0.11	4.918	+0.14	2057	94.5	+0.32	4.890	-0.27	2085
94.0	0	4.916	+0.10	2084	94.4	+0.21	4.892	-0.22	2050
93.7	-0.32	4.923	+0.24	2039	94.4	+0.21	4.893	-0.20	2070
93.5	-0.53	4.939	+0.55	2088	94.6	+0.42	4.888	-0.31	2085
94.2	+0.21	4.903	-0.16	2093	93.8	-0.42	4.921	+0.37	2098
94.6	+0.64	4.886	-0.51	2089	94.0	-0.21	4.912	+0.18	2092
94.9	+0.96	4.878	-0.67	2089	93.9	-0.32	4.922	+0.39	2092
94.6	+0.64	4.880	-0.63	2088	93.8	-0.42	4.922	+0.39	2092
94.0		4.911		2076	94.2		4.903		2082
0.555		0.0231		17.8	0.297		0.0145		14.3
5.90×10^{-3}		4.70×10^{-3}		8.56×10^{-3}	3.15×10^{-3}		2.97×10^{-3}		6.86×10^{-3}

Lamp No. 7S					Lamp No. 8S				
V(V)	%	I(A)	%	T_c(K)	V(V)	%	I(A)	%	T_c(K)
101.1	-0.49	4.599	+0.33	2055	100.2	-0.10	4.639	-0.04	2066
101.7	+0.10	4.571	-0.28	2064	100.3	0	4.638	-0.06	2055
101.3	-0.30	4.595	+0.24	2067	100.3	0	4.636	-0.11	2073
101.3	-0.30	4.600	+0.35	2027	100.7	+0.40	4.624	-0.37	2069
102.6	+0.98	4.539	-0.98	2057	100.7	+0.40	4.626	-0.32	2085
101.4	-0.20	4.598	+0.31	2075	100.5	+0.20	4.635	-0.13	2073
101.5	-0.10	4.590	+0.13	2075	100.0	-0.30	4.656	+0.32	2085
101.7	+0.10	4.587	-0.07	2083	99.9	-0.40	4.660	+0.41	2092
101.8	+0.20	4.581	-0.07	2076	100.3	0	4.644	+0.06	2082
101.8	+0.20	4.578	-0.13	2074	100.2	-0.10	4.649	+0.17	2079
101.6		4.584		2065	100.3		4.641		2075
0.418		0.0185		16.1	0.264		0.0118		10.6
4.12×10^{-3}		4.04×10^{-3}		7.81×10^{-3}	2.64×10^{-3}		2.54×10^{-3}		5.09×10^{-3}

Table V. (Continued)

Lamp No. 9S					Lamp No. 10S				
V(V)	%	I(A)	%	T_c(K)	V(V)	%	I(A)	%	T_c(K)
106.0	+1.34	4.414	-1.54	2041	101.5	0	4.583	-0.13	2090
104.3	-0.29	4.471	-0.27	2079	101.5	0	4.581	-0.17	2086
103.8	-0.76	4.497	+0.31	2063	101.0	-0.49	4.608	+0.41	2069
104.4	-0.19	4.476	-0.16	2053	101.6	+0.10	4.586	-0.07	2047
103.8	-0.76	4.492	+0.20	2081	101.5	0	4.588	-0.02	2075
104.3	-0.29	4.480	-0.07	2074	101.3	-0.20	4.596	+0.15	2081
104.0	-0.57	4.490	+0.16	2078	101.2	-0.30	4.599	+0.22	2078
103.9	-0.67	4.502	+0.42	2085	101.8	+0.30	4.579	-0.22	2087
103.8	-0.76	4.501	+0.40	2068	101.8	+0.30	4.577	-0.26	2067
103.5	-1.05	4.511	+0.62	2075	101.4	-0.10	4.590	+0.02	2079
104.2		4.483		2070	101.5		4.589		2076
0.699		0.0274		13.8	0.250		0.0098		12.6
6.71×10^{-3}		6.11×10^{-3}		6.67×10^{-3}	2.47×10^{-3}		2.14×10^{-3}		6.07×10^{-3}

Lamp No. 11S					Lamp No. 12S				
V(V)	%	I(A)	%	T_c(K)	V(V)	%	I(A)	%	T_c(K)
101.7	+0.20	4.569	-0.33	2084	103.8	-0.10	4.501	+0.02	2022
101.7	+0.20	4.569	-0.33	2047	103.6	-0.29	4.505	+0.11	2052
101.8	+0.30	4.569	-0.33	2082	103.5	-0.39	4.512	+0.27	2040
101.2	-0.30	4.597	+0.28	2052	104.7	+0.77	4.474	-0.58	2086
100.8	-0.69	4.607	+0.50	2044	104.5	+0.58	4.479	-0.47	2086
100.7	-0.79	4.614	+0.65	2075	104.4	+0.48	4.480	-0.44	2072
100.7	-0.79	4.618	+0.74	2079	103.8	-0.10	4.506	+0.13	2076
101.9	+0.34	4.575	-0.20	2074	103.6	-0.29	4.514	+0.31	2081
102.3	+0.79	4.557	-0.59	2084	103.5	-0.39	4.519	+0.42	2064
102.1	+0.59	4.562	-0.48	2064	103.6	-0.29	4.513	+0.29	2076
101.5		4.584		2069	103.9		4.500		2066
0.595		0.0229		15.6	0.455		0.0165		20.3
5.86×10^{-3}		5.00×10^{-3}		7.56×10^{-3}	4.38×10^{-3}		3.67×10^{-3}		9.81×10^{-3}

Table VI. Total luminous fluxes Φ_V and the correlated color temperature of 12 stable HPS lamps.

Lamp No.	Φ_V(lm)	T_c (K)
1	51480	2080
2	49310	2090
3	51010	2080
4	50410	2070
5	51500	2080
6	51650	2080
7	49780	2070
8	50430	2080
9	50320	2070
10	50060	2080
11	49000	2070
12	47710	2070

References

[1]   Louden, W.C. and Schmidt, K., "High pressure sodium discharge arc lamps" Ill. Eng. 60 (12), 696, (1965).

[2]   Otani, K., Kawahara, K., Watanabe, K., and Tsuchihashi, M., "A high pressure sodium lamp with improved color rendition" Journal of IES 11 (7), 237, (1982).

[3]   McVey, C.I., "High Pressure sodium lamp technology" IEEE Proc., 127, pt. A (3), 158, (1980).

[4]   Wharmby, D.O., "Scientific aspects of the high pressure sodium lamp" ibid, 127 pt. A (3), 165, (1980).

[5]   Van Vliet, J.A.J.M. and de Groot, J.J., "High pressure sodium discharge lamp" ibid., 128, pt. A (6), 145, (1981).

[6]   Akutsu, H., "Trends in HPS lamp technology" Lighting Research and technology 16 (2), 73, (1984).

[7]   International Commission on Illumination (CIE), "Method of measuring and specifying color rendering properties of light sources" CIE Publ. no. 13, 2 (TC-3.2) (1974).

[8]   Bhalla, R.S., Larson, D.A., and Unglert, M.C., "HPS lamp with improved color rendering" Journal of IES 8 (7), 202, 979).

[9]   Akutsu, H., Watarai, Y., Saito, N., and Mizuno, H., " A new high pressure sodium lamp with high colour acceptability" Journal of IES 13 (7), 341, (1984).

[10]   Denbigh, P.L., "Effect of sodium/mercury ratio and amalgam temperature efficacy of 400 W HPS lamps" Lighting Research and Technology 6 (2), 62, (1974).

[11]   See for example:
        Waymouth, J.F., "An elementary model of the high-pressure sodium lamp" Journal of IES 6 (3), 131, (1977).

        Akutsu, H. and Saito, N., "Energy balance of a high-pressure sodium arc tube" Journal of Light and Visual Environment" 3, 11, 1979.

[12]   Waymouth, J.F. and Wyner, E.F., "Analysis of factors affecting efficacy of HPS lamps" Journal of IES 10 (4), 237, (1981).

[13]   Jacobs, C.A.J., Sprengers, L. and de Vaan, R.L.C., "Arc voltage control in low and high pressure sodium lamps" Journal of IES 7 (1), 125, (1978).

[14] Li, S.Z., Zhou, T.M., and Cai, Z.Q., "Analysis of factors affecting the color rendition of HPS lamps" Proceedings of meeting on High temperature lamp chemistry, Electric Chemistry Society (China) (1985) (Edited by Zubler, E.G.)

[15] See for example:
      Wyner, E., "Electrolysis of sodium through alumina arc tubes" Journal of IES $\underline{8}$ (3), 166, 1979.

[16] "Specification for 400W HPS lamps S51" ANSI C78.1350-1976. "HPS lamps - method of measuring characteristics" ANSI C78.388 - 1984.

[17] "Lamp Testing Engineer's Conference (LTEC)" Meeting in NBS, September 25, 1985.

[18] "Procedures for the measurement of luminous flux of discharge lamps and for their calibration as working standards" CIE Publication No. 25 (1973, Reprinted 1982).

[19] "The spectroradiometric measurement of light sources" CIE Publication No. 63, (1984).

[20] See for example:
      McSparron, D.A., Mohan, K., Raybold, R.C., Saunders, R.D. and Zalewski, E.F., "Spectroradiometry and conventional photometry - An interlaboratory comparison" NBS Technical Note 559, 1970;

      Nonaka, M., Kinameri, K., and Ishiba, M., "Spectroradiometric measurement on fluorescent lamps" Metrologia $\underline{8}$ (4), 133, (1972);

      Spears, G.R., "Spectroradiometry Photometry" Journal of IES $\underline{3}$ (3), 229, (1974).

[21] "Specification for HID lamp reference ballasts" ANSI C82.5-1977.

[22] Mielenz, K.D. and Eckerle, K.L., "Spectrophotometer linearity testing using the double-aperture method" Appl. opt. $\underline{11}$ (10), 2294, (1972).

[23] Booker, R.L. and McSparron, D.A., "Photometric Calibration Services at NBS", Nat. Bur. Stand (U.S.), Spec. Publ. 250-15 (1987).

[24] "IES approved method for photometric measurements of HID lamps", Journal of the IES $\underline{4}$ (3), 229, (1975).

U.S. DEPT. OF COMM. **BIBLIOGRAPHIC DATA** **SHEET** *(See instructions)*	**1.** PUBLICATION OR REPORT NO. NBS/TN-594/14	**2.** Performing Organ. Report No.	**3.** Publication Date August 1988

4. TITLE AND SUBTITLE

HIGH PRESSURE SODIUM DISCHARGE LAMP CHARACTERIZATION FOR USE AS STANDARDS OF GEOMETRICALLY TOTAL LUMINOUS FLUX

5. AUTHOR(S)

Minggao He and Robert J. Bruening

6. PERFORMING ORGANIZATION *(If joint or other than NBS, see instructions)* **NATIONAL BUREAU OF STANDARDS** **U.S. DEPARTMENT OF COMMERCE** **GAITHERSBURG, MD 20899**	**7.** Contract/Grant No.
	8. Type of Report & Period Covered Final

9. SPONSORING ORGANIZATION NAME AND COMPLETE ADDRESS *(Street, City, State, ZIP)*

SAME AS ITEM #6 ABOVE.

10. SUPPLEMENTARY NOTES

☐ Document describes a computer program; SF-185, FIPS Software Summary, is attached.

11. ABSTRACT *(A 200-word or less factual summary of most significant information. If document includes a significant bibliography or literature survey, mention it here)*

The stability of commercial 400W high pressure sodium lamps has been studied to allow the selection of lamps that produce a stable luminous flux on relighting. The properties of the lamps have been studied during the first minutes of starting, their output on relighting in place, and their output after 100's of hours burning. Lamps have been selected that repeat to ± 1% on relighting, and are expected to remain that stable over a life of about 450 hours. The lamps have been calibrated for total luminous flux by sphere comparison, with an uncertainty of ±4.6%. These lamps will be used as working standards, and goniometric measurements will be made to reduce the uncertainty.

12. KEY WORDS *(Six to twelve entries; alphabetical order; capitalize only proper names; and separate key words by semicolons)*

high pressure sodium lamps; stability of HPS lamps; standard spectral flux lamps

13. AVAILABILITY ☒ Unlimited ☐ For Official Distribution. Do Not Release to NTIS ☒ Order From Superintendent of Documents, U.S. Government Printing Office, Washington, D.C. 20402. ☐ Order From National Technical Information Service (NTIS), Springfield, VA. 22161	**14.** NO. OF PRINTED PAGES 49
	15. Price

NBS Technical Publications

Periodical

Journal of Research—The Journal of Research of the National Bureau of Standards reports NBS research and development in those disciplines of the physical and engineering sciences in which the Bureau is active. These include physics, chemistry, engineering, mathematics, and computer sciences. Papers cover a broad range of subjects, with major emphasis on measurement methodology and the basic technology underlying standardization. Also included from time to time are survey articles on topics closely related to the Bureau's technical and scientific programs. Issued six times a year.

Nonperiodicals

Monographs—Major contributions to the technical literature on various subjects related to the Bureau's scientific and technical activities.

Handbooks—Recommended codes of engineering and industrial practice (including safety codes) developed in cooperation with interested industries, professional organizations, and regulatory bodies.

Special Publications—Include proceedings of conferences sponsored by NBS, NBS annual reports, and other special publications appropriate to this grouping such as wall charts, pocket cards, and bibliographies.

Applied Mathematics Series—Mathematical tables, manuals, and studies of special interest to physicists, engineers, chemists, biologists, mathematicians, computer programmers, and others engaged in scientific and technical work.

National Standard Reference Data Series—Provides quantitative data on the physical and chemical properties of materials, compiled from the world's literature and critically evaluated. Developed under a worldwide program coordinated by NBS under the authority of the National Standard Data Act (Public Law 90-396).
NOTE: The Journal of Physical and Chemical Reference Data (JPCRD) is published quarterly for NBS by the American Chemical Society (ACS) and the American Institute of Physics (AIP). Subscriptions, reprints, and supplements are available from ACS, 1155 Sixteenth St., NW, Washington, DC 20056.

Building Science Series—Disseminates technical information developed at the Bureau on building materials, components, systems, and whole structures. The series presents research results, test methods, and performance criteria related to the structural and environmental functions and the durability and safety characteristics of building elements and systems.

Technical Notes—Studies or reports which are complete in themselves but restrictive in their treatment of a subject. Analogous to monographs but not so comprehensive in scope or definitive in treatment of the subject area. Often serve as a vehicle for final reports of work performed at NBS under the sponsorship of other government agencies.

Voluntary Product Standards—Developed under procedures published by the Department of Commerce in Part 10, Title 15, of the Code of Federal Regulations. The standards establish nationally recognized requirements for products, and provide all concerned interests with a basis for common understanding of the characteristics of the products. NBS administers this program as a supplement to the activities of the private sector standardizing organizations.

Consumer Information Series—Practical information, based on NBS research and experience, covering areas of interest to the consumer. Easily understandable language and illustrations provide useful background knowledge for shopping in today's technological marketplace.
Order the above NBS publications from: Superintendent of Documents, Government Printing Office, Washington, DC 20402.
Order the following NBS publications—FIPS and NBSIR's—from the National Technical Information Service, Springfield, VA 22161.

Federal Information Processing Standards Publications (FIPS PUB)—Publications in this series collectively constitute the Federal Information Processing Standards Register. The Register serves as the official source of information in the Federal Government regarding standards issued by NBS pursuant to the Federal Property and Administrative Services Act of 1949 as amended, Public Law 89-306 (79 Stat. 1127), and as implemented by Executive Order 11717 (38 FR 12315, dated May 11, 1973) and Part 6 of Title 15 CFR (Code of Federal Regulations).

NBS Interagency Reports (NBSIR)—A special series of interim or final reports on work performed by NBS for outside sponsors (both government and non-government). In general, initial distribution is handled by the sponsor; public distribution is by the National Technical Information Service, Springfield, VA 22161, in paper copy or microfiche form.

Stimulating America's Progress
1913-1988